Quaternary Science Reviews 257 (2021) 106838

Contents lists available at ScienceDirect

Quaternary Science Reviews

journal homepage: www.elsevier.com/locate/quascirev

The first continuous late Pleistocene tephra record from Kamchatka Peninsula (NW Pacific) and its volcanological and paleogeographic implications

Vera Ponomareva [a, *], I. Florin Pendea [b], Egor Zelenin [c], Maxim Portnyagin [d, e], Natalia Gorbach [a], Maria Pevzner [c], Anastasia Plechova [e], Alexander Derkachev [f], Alexey Rogozin [a], Dieter Garbe-Schönberg [g]

[a] Institute of Volcanology and Seismology, Piip Boulevard 9, Petropavlovsk-Kamchatsky, 683006, Russia
[b] Lakehead University, Sustainability Sciences Department, 500 University Avenue, Orillia, ON, L3V0B9, Canada
[c] Geological Institute, Pyzhevsky Lane 7, Moscow, 119017, Russia
[d] GEOMAR Helmholtz Center for Ocean Research Kiel, Wischhofstrasse 1-3, 24148, Kiel, Germany
[e] V.I. Vernadsky Institute of Geochemistry and Analytical Chemistry, Kosygin St. 19, Moscow, 119991, Russia
[f] V.I. Il'ichev Pacific Oceanological Institute, 43 Baltiyskaya St, Vladivostok, 690041, Russia
[g] Institute of Geosciences, Kiel University, Ludewig-Meyn-Strasse 10, 24118, Kiel, Germany

ARTICLE INFO

Article history:
Received 14 June 2020
Received in revised form
31 January 2021
Accepted 5 February 2021
Available online 25 February 2021

Handling Editor: Giovanni Zanchetta

Keywords:
Tephra
Explosive eruption
Volcanic glass composition
Electron microprobe
LAICP-MS
Kamchatka peninsula
NW Pacific
Late pleistocene
Proglacial lake
Glaciation

ABSTRACT

The Kamchatka volcanic arc (NW Pacific) is one of the most productive arcs in the world, known for its highly explosive activity. At the same time, the Kamchatkan record of late Pleistocene explosive eruptions has remained fragmentary. Here we present the first continuous record of Kamchatkan explosive activity between ~12 and 30 ka, which includes ~70 eruptions and extends the earlier reconstructed Holocene sequence for another 20 ka. Our record is based on geochemical correlations of ^{14}C-dated tephras that represent all Kamchatka volcanic zones and are buried in lacustrine deposits along the 200 km stretch of the Central Kamchatka Depression (CKD). The accompanying geochemical database of volcanic glass compositions includes 3104 new electron microprobe and 221 LA-ICP-MS analyses. The data show that during the period under study, large silicic explosive eruptions peaked at 30–25 ka. Later times were mostly associated with moderate activity from northern CKD volcanoes Shiveluch and Zarechny. Our tephra record provides the first tephrochronological model for dating and correlating Central Kamchatka late Pleistocene deposits and gives us some insight into the timing of glacial advances in the Kliuchevskoi volcanic group and volcanic response to the onset of the Last Glacial Maximum and glacial unloading at its termination. In addition, studied sections of lacustrine deposits tightly linked by tephra markers suggest the existence of a large lake system within the CKD for ~20 kyr until its final discharge at ~12 ka BP.

1. Introduction

Research on temporal patterns in volcanic activity and its interaction with paleoenvironmental changes requires continuous and well dated eruptive records. For late Pleistocene times, well-resolved terrestrial records are available for only some regions, e.g., Chilean Lake District (Fontijn et al., 2016), Japan (Albert et al., 2019), interior Alaska and Yukon (Davies et al., 2016). Here we present the first late Pleistocene tephra record for the Kamchatka volcanic arc (NW Pacific), one of the most productive arcs in the world, known for its highly explosive eruptions (Braitseva et al., 1995; Bindeman et al., 2010; Ponomareva et al., 2004, 2013a). Kamchatka cryptotephras have been identified in North America (Mackay et al., 2016), Greenland (Cook et al., 2018), and Svalbard (van der Bilt et al., 2017), which demonstrates the hemispheric

* Corresponding author.
E-mail addresses: vera.ponomareva1@gmail.com (V. Ponomareva), ifpendea@lakeheadu.ca (I.F. Pendea), egorzelenin@mail.ru (E. Zelenin), mportnyagin@geomar.de (M. Portnyagin), n_gorbach@mail.ru (N. Gorbach), m_pevzner@mail.ru (M. Pevzner), aplech@gmail.com (A. Plechova), derkachev@poi.dvo.ru (A. Derkachev), alekseiras@yandex.ru (A. Rogozin), schoenberg@ifg.uni-kiel.de (D. Garbe-Schönberg).

https://doi.org/10.1016/j.quascirev.2021.106838
0277-3791/

impact of the Kamchatka eruptions and highlights the importance of Kamchatka tephra research. Numerous Holocene Kamchatkan tephras have been described and dated (e.g., Braitseva et al., 1995, 1997; Bazanova et al., 2005; Kyle et al., 2011; Pevzner, 2015; Pinegina et al., 2018, 2020; Ponomareva et al., 2004, 2013b, 2015, 2017), while older, pre-Holocene, tephra sequences were considered to have been largely eroded during the Pleistocene glaciations (Braitseva et al., 1995). A few outcrops exhibiting fragmentary Pleistocene tephra records were described in the central part of the Central Kamchatka Depression (CKD; Braitseva et al., 1968; Kuprina, 1970), however, only a few bulk tephras from these outcrops have been analyzed for major element composition (Kirianov, 1981; Braitseva et al., 2005). As a result, our current understanding of the scale and temporal patterns of the late Pleistocene explosive eruptions in Kamchatka is based on a small number of dated ignimbrites and on a few tephras of unknown stratigraphic order (Braitseva et al., 1995, 2005; Bindeman et al., 2010). The first continuous late Pleistocene record of the Kamchatka tephras has been recently reported from the marine core ~400 km east of Kamchatka (Derkachev et al., 2020). However, this record is poorly resolved, about a half of its twenty one tephra layers have mixed glass populations probably resulting from low sediment accumulation rate that hampers the understanding of the eruption sequence. A marine tephra record west of Kamchatka, in the Okhotsk Sea, does not contain any late Pleistocene Kamchatka tephras (Derkachev et al., 2016). A drill core from the Chukotka El'gygytgyn Lake north of Kamchatka contains only one late Pleistocene tephra (T0) provisionally assigned to a Kamchatkan volcano (van den Bogaard et al., 2014).

Here we present the first continuous and detailed terrestrial late Pleistocene tephra record for the Kamchatka Peninsula, which starts from ~30 ka BP and extends to the Holocene. The record is preserved in lacustrine deposits within the modern Kamchatka River valley and its tributaries, and is exposed in a number of natural outcrops and man-made excavations spanning a distance of ~200 km along the Central Kamchatka Depression (Fig. 1). We geochemically fingerprint glass from ~70 tephras with ~3000 electron microprobe analyses for major and some volatile elements and, additionally, glass from fifteen major marker tephras with 192 single-shard LA-ICP-MS analyses for trace elements. These efforts have allowed us to correlate individual tephra layers among the studied sections. The chronological framework for the tephra layers is based on eleven ^{14}C dates and subsequent Bayesian age modeling. The studied tephra sequences provide the first continuous record of the Kamchatka explosive volcanism for this period and allow us to consider the changes in the eruptive activity during the times of glacial unloading. In addition, tephra correlations among disparate lacustrine deposits over a large area in the Central Kamchatka Depression allow us to preliminary hypothesize an existence of a glacial lake system spanning ~20 kyr.

2. Study area

The Kamchatka Peninsula overlies the northwestern margin of the subducting Pacific plate and is one of the most volcanically and tectonically active regions in the world (e.g., Gorbatov et al., 1997). The first-order elements of the present-day topography are the CKD, and Sredinny and East Kamchatka Ranges bounding the CKD from the west and east, respectively (Fig. 1). Kamchatka hosts about 30 active volcanoes and hundreds of monogenetic vents grouped into two major volcanic belts running SW-NE along the peninsula: the Eastern Volcanic Belt (EVB) and Sredinny Range (SR, Fig. 1).

EVB includes three segments: southern (51–53° N), central (53–55° N), and northern (55-57.5° N). In the southern and central segments, the belt runs for ~500 km parallel to the trench. These segments of EVB are often collectively referred to as the Eastern Volcanic Front (EVF, e.g., Churikova et al., 2001). In this work, following Portnyagin et al. (2020), we distinguish the volcanic front (VF) and rear-arc (RA) volcanoes in these parts of the volcanic belt. At 55° N, EVB deviates to the northwest to form the northern segment, which includes the most voluminous volcanic cluster of the Kamchatka arc, the Kliuchevskoi volcanic group, and Zarechny, Kharchinsky, and Shiveluch volcanoes farther north (Figs. 1 and 2A), which collectively are known as the Central Kamchatka Depression (CKD) volcanoes.

The Kliuchevskoi volcanic group consists of active Kliuchevskoi, Bezymianny, Plosky Dalny (Ushkovsky), and Plosky Tolbachik volcanoes, as well as ten dormant or extinct large eruptive centers and numerous small vents (Figs. 1 and 2A). All the high elevation (up to ~4850 m a.s.l.) volcanoes of Kliuchevskoi group were constructed during the late Pleistocene or Holocene (Melekestsev et al., 1974; Braitseva et al., 1995). Kharchinsky is a partly eroded extinct volcano with the superimposed chain of late Pleistocene cinder cones (Volynets et al., 1999a). Zarechny volcano sitting on the Kharchinsky southern slope, is a complex late Pleistocene edifice consisting of a large cone (Zarechny I), which hosts a large collapse crater, a smaller inner cone and lava dome (Zarechny II) estimated to have formed during the Last Glacial Maximum (LGM) (Fig. 2B; Volynets et al., 1999a). Shiveluch is a giant complex edifice consisting of the Pleistocene Old Shiveluch volcano, destroyed by a collapse crater, and the currently active Young Shiveluch (YSH) eruptive center nested in the latter. Southwestern part of Old Shiveluch is known as Baidarny Spur (Gorbach et al., 2013) with the activity extending into the Late Glacial times (Pevzner et al., 2013). Most of the Kliuchevskoi group volcanic products are basalts - basaltic andesites and trachyandesites with a subordinate amount of andesites. Kharchinsky and Zarechny rocks are dominantly basalts with minor andesites (Volynets et al., 1999b). Shiveluch rocks are predominantly andesites with subordinate amount of more mafic varieties (Melekestsev et al., 1991b; Volynets et al., 1997; Gorbach et al., 2013). No rhyolite rocks have ever been reported for the CKD volcanoes.

Nowadays Kamchatka hosts about 500 small glaciers, covering a total area of ~900 km^2 (Solomina et al., 2007), including the glaciers on the highest CKD volcanoes (Fig. 1). Widely distributed moraine and offshore ice-rafted debris (IRD) layers attest to former existence of extensive ice masses in Kamchatka (Fig. 2A; Braitseva et al., 1968; Melekestsev et al., 1974; Bigg et al., 2008; Nürnberg et al., 2011; Barr and Clark, 2012; Barr and Solomina, 2014). In our study area, a large glacier originated in the debris-avalanche crater of Shiveluch volcano and descended its southern slope for >50 km to the foothills of the Kliuchevskoi group (Melekestsev et al., 1974) (Fig. 2A and B). Glacial till and glaciofluvial deposits related to the melting of this glacier are composed of typical Shiveluch material and outcrop near Kliuchi village (Fig. 2B). Another large glacier descended the Studenaya-Pakhcha river valley in the western part of the Kliuchevskoi volcanc group (Fig. 2C). The study area is drained by the Kamchatka River and its tributaries (Fig. 1). The river valley is wide and, in addition to the main river channel, hosts numerous lakes and minor branches (Fig. 2B and C).

Holocene volcanic and related debris fan deposits occupy the slopes of active volcanoes (Fig. 1). All the terrain is mantled by the Holocene soil-pyroclastic sequence composed of alternating tephra and paleosol/silt layers. The cover is 2–3 m thick in the Kamchatka River valley 30–50 km away from active volcanoes, and thickens up to 12–20 m at a distance of 15 km. The Holocene cover in our study area overlies glacial till and lacustrine deposits.

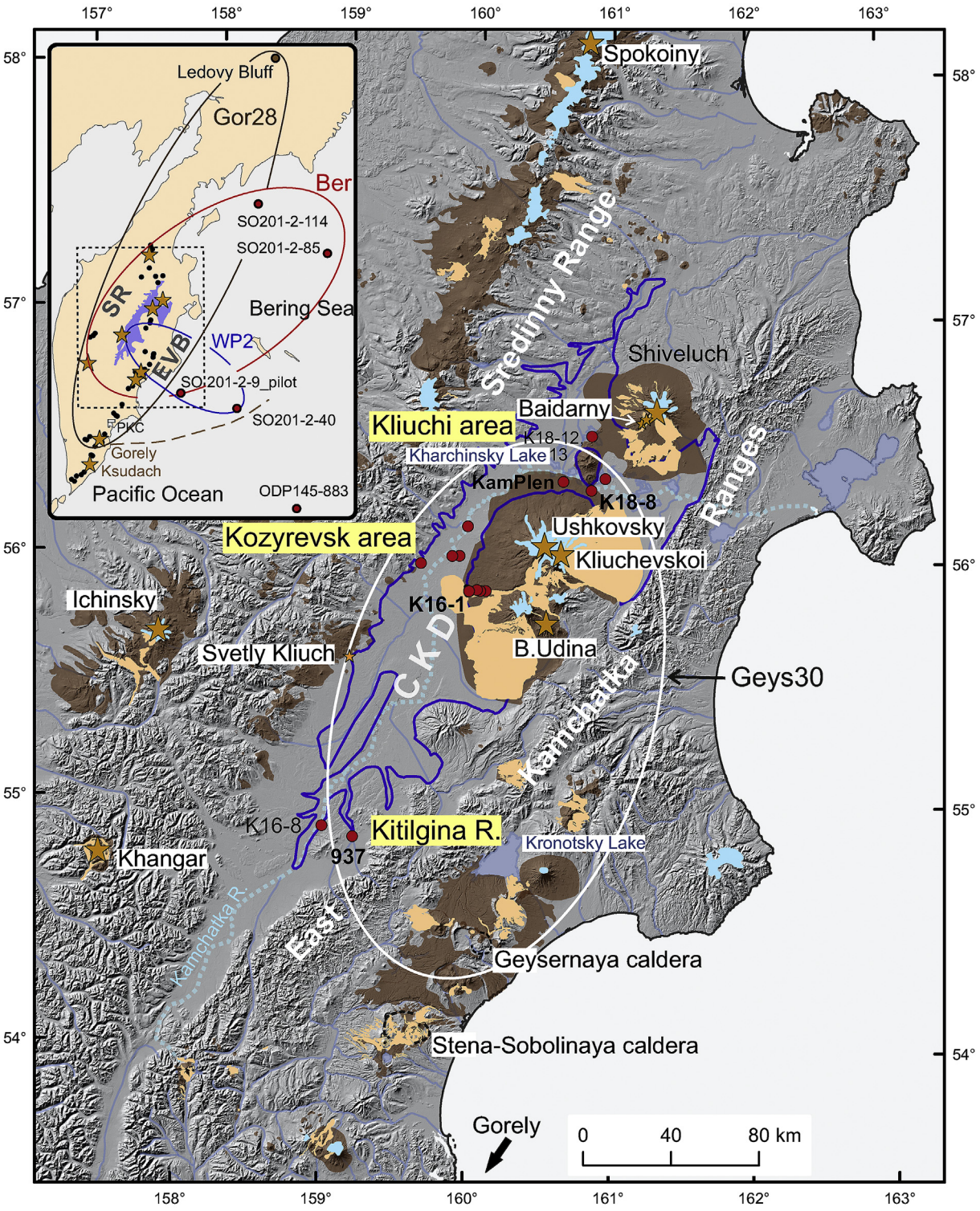

Fig. 1. Location map showing study areas (highlighted in yellow), measured sections (red circles, key sites labeled in bold), and suggested extent of the CKD lake basin (blue outline in the figure and blue shade in the inset). Modern glaciers are shown in turquoise, Holocene volcanic deposits including debris fans are in light brown, late Pleistocene volcanic deposits are in dark brown. The white oval shows approximate dispersal of the *Geys30* tephra. **Inset** shows distal tephra sites (red circles) and suggested minimum dispersal areas for major tephra markers (colored ovals): red – tephra *Ber*, brown – *Gor28*; blue – *WP2*. (For interpretation of the references to color in this figure legend, the reader is referred to the Web version of this article.)

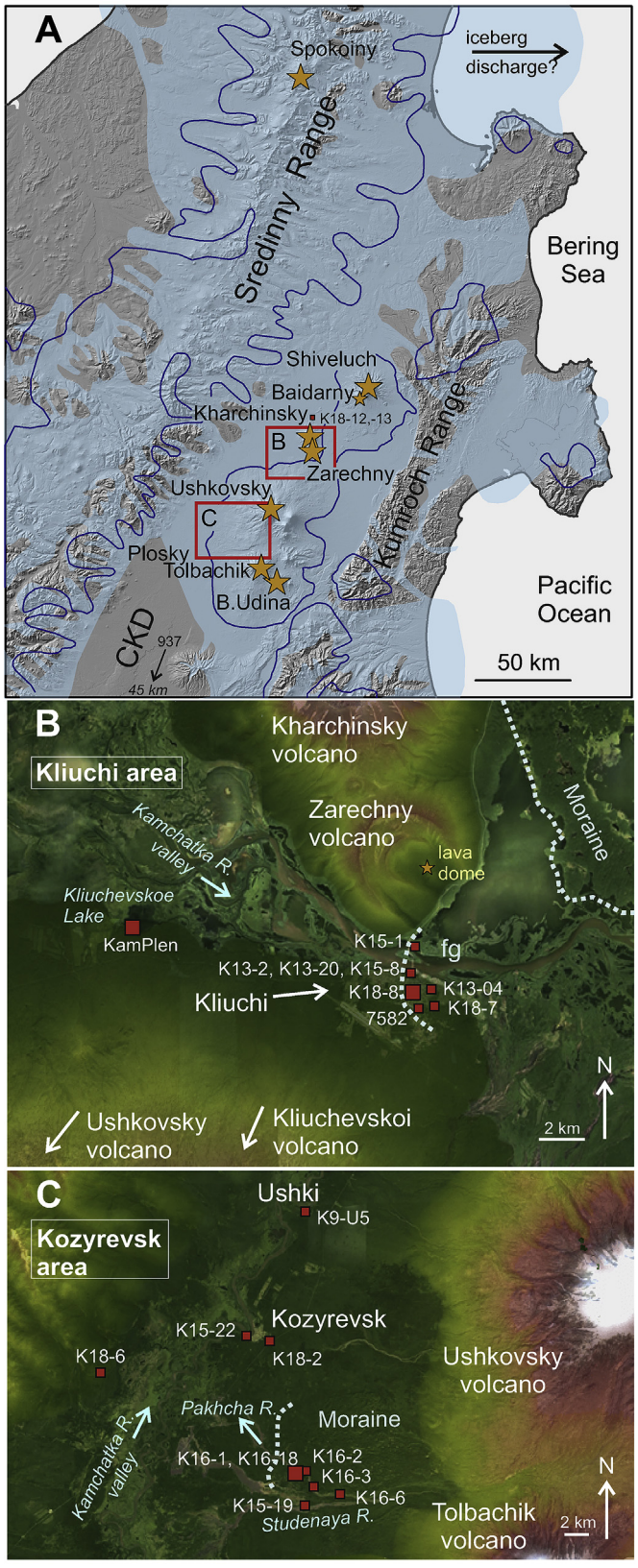

Fig. 2. Detailed location map of the Kliuchi and Kozyrevsk study areas. **A.** Presumed extent of glaciers of stages I (light-blue shading; according to Melekestsev, 1974) and II (dark-blue outline; according to Barr and Clark, 2012, with additions from Braitseva et al., 1968) of the late Pleistocene glaciation. Stage I is roughy dated at 60–31 ka and Stage II is thought to correlate to the global LGM (Barr and Solomina, 2014). Late Pleistocene volcanoes mentioned in the text are labeled (B. Udina = Bolshaya Udina). Kliuchi and Kozyrevsk study areas are shown in red rectangles. **B** and **C.** Kliuchi and Kozyrevsk study areas, respectively. Measured sections are shown with red squares, key sites KamPlen and K18-8 (in **B**) and K16-1 (in **C**) - with larger ones. Western outlines of glaciofluvial deposits and the till related to the Shiveluch glacier, as well as the moraine field in the Pakhcha valley, are shown with light-blue dotted lines and labeled; Fg - glaciofluvial. (For interpretation of the references to color in this figure legend, the reader is referred to the Web version of this article.)

3. Materials and methods

3.1. Sites and samples

Our sites, where most of the tephras were geochemically fingerprinted, are located along the Kamchatka River valley, from the Kharchinsky Lake in the north to Kitilgina River in the south (Fig. 1). The sites are located in three major areas (from north to south): Kliuchi area, Kozyrevsk area, and Kitilgina River area (Fig. 1). The key sections of tephra-bearing lacustrine deposits extending down to ~28–30 ka are KamPlen and K18-8 in the Kliuchi area (Fig. 2B), K16-1 (=K16-18) in the Kozyrevsk area (Figs. 2C), and 937 in the Kitilgina River area (Fig. 1). In twelve additional excavations, only the upper parts of lacustrine deposits were unearthed and selective tephras analyzed. Additionally, we analyzed tephras in four more sites in Kliuchi town and across the Kamchatka River, at Zarechny slope (Figs. 1 and 2B). The sections were measured and sampled in 2013–2019. Major stratigraphic sections are provided in Figs. 3 and 4; photos of selected key sections in Figs. 5–6, and the details of tephra stratigraphy, grainsize, and color in each of the sections are provided in Supplement 1. Additional photos and descriptions of the tephra-bearing deposits as well as tephra sample IDs are provided in Supplement 2. All visible tephra layers in each of the sections were labeled consecutively from top to bottom (site prefix-serial number) (Figs. 3 and 4; Supplements 1–4).

3.2. Geochemical and mineralogical studies

Geochemical and mineralogical studies included electron microprobe (EMP) and laser ablation inductively coupled mass spectrometric (LA-ICP-MS) analyses of volcanic glass and examination of KamPlen tephras with an optical microscope. We obtained major element geochemistry from 155 tephra samples collected in 23 sections (Supplement 3). In addition, 128 more glass analyses from our database were used for tracing selected major tephras beyond the study area; these earlier unpublished reference analyses are also included in Supplement 3. EMP analyses were performed at GEOMAR (Kiel, Germany) during 36 analytical sessions between 2008 and 2020. Volcanic glass was analyzed using the JEOL JXA 8200 wavelength dispersive electron microprobe. The analytical conditions for glasses were 15 kV accelerating voltage, 6 nA current and 5 μm electron beam size. Details of the analytical technique are provided by Portnyagin et al. (2020). Data on EMP reference materials obtained in the course of this study are listed in Supplement 3.

LA-ICP-MS analyses of major and trace elements in marker tephras and some reference glasses used for distal correlations were carried out at the Institute of Geosciences at Kiel University (Kiel, Germany). The analyses were obtained using a Coherent GeoLas HD ArF 193 nm excimer LA system coupled with quadrupole-based ICP-MS Agilent 7500s (2010–2016) and Agilent 7900 (2017–2020). The majority of the analyses were obtained using the high sensitivity Agilent 7900 instrument, laser spot size of 24 μm, pulse frequency of 10 Hz, and fluence of 5 J cm^{-1}. These recent analyses included all major elements (Si, Ti, Al, Fe, Mn, Mg, Ca, Na, K, P), and the data were quantified by adjusting the sum of major elements to 100 wt%, allowing direct comparison with EPMA

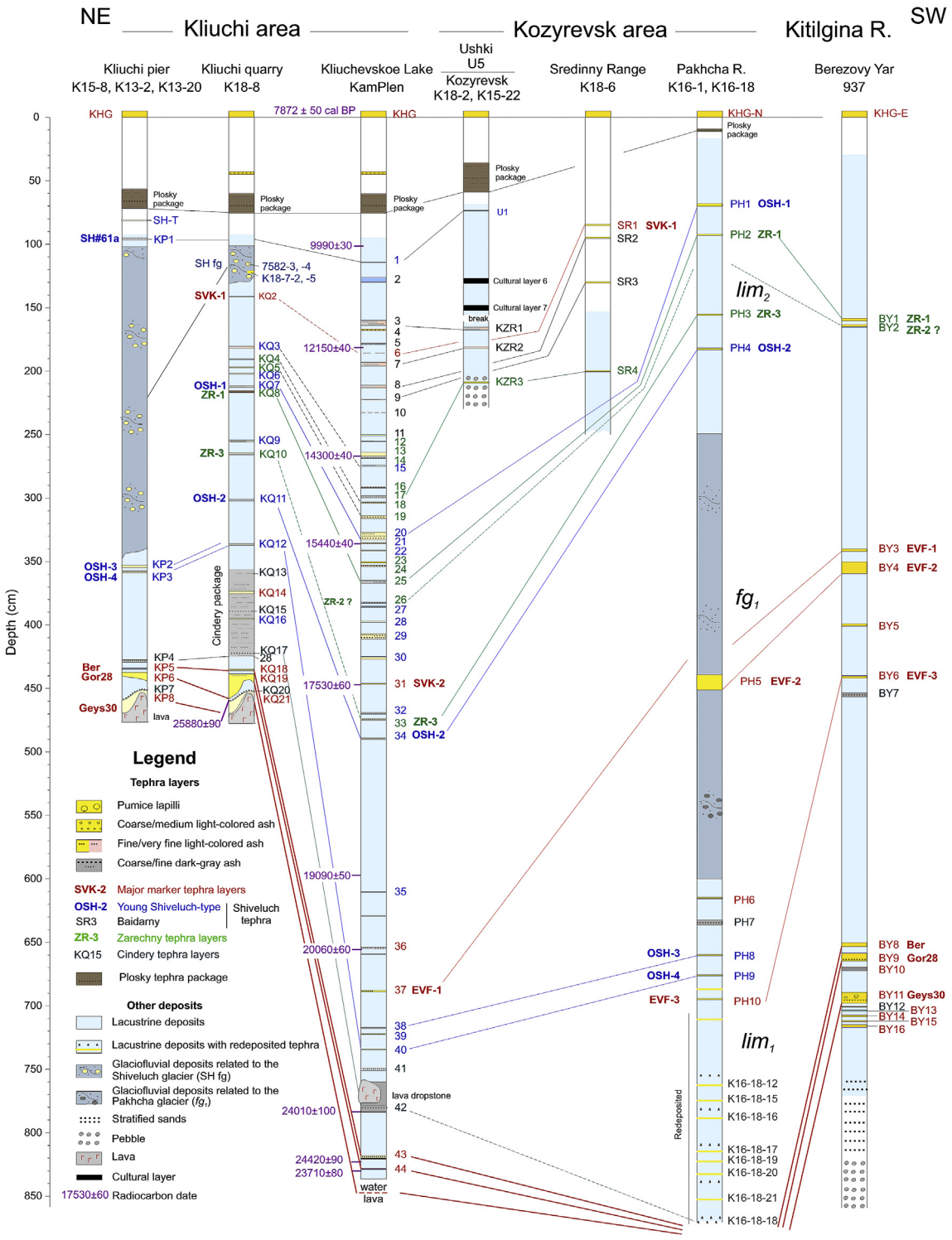

Fig. 3. Graphic representation of key measured sections through the lacustrine and glacial deposits in the study area; for location of the sections see Figs. 1 and 2. Each tephra layer is labeled with tephra code in the individual sections (right of each column; samples in KamPlen have the site name as prefix); in addition, major markers are labeled with individual codes. Sample IDs can be found in Supplement 2. Tephra IDs and correlation lines are color-coded: red – major (bold) or potential tephra markers, blue – Shiveluch tephra, green – Zarechny, black – Baidarny, dark-green – mafic cinders from various sources. KHG – Holocene marker tephra from Khangar volcano (Braitseva et al., 1997; Cook et al., 2018); Plosky package – set of cindery tephra layers related to the early Holocene activity from fissure zone superimposed on the Plosky volcanic massif (Ponomareva et al., 2013b). Sample IDs at the bottom of section K16-1 are from light-colored glass-rich silt layers. SH fg - glaciofluvial deposits related to the Shiveluch glacier. Deposits in the Pakhcha valley are labeled following Kraevaya and Kuralenko (1983): lim_1 and lim_2 - lacustrine deposits; fg_1 - glaciofluvial deposits of the stage I of the late Pleistocene glaciation. (For interpretation of the references to color in this figure legend, the reader is referred to the Web version of this article.)

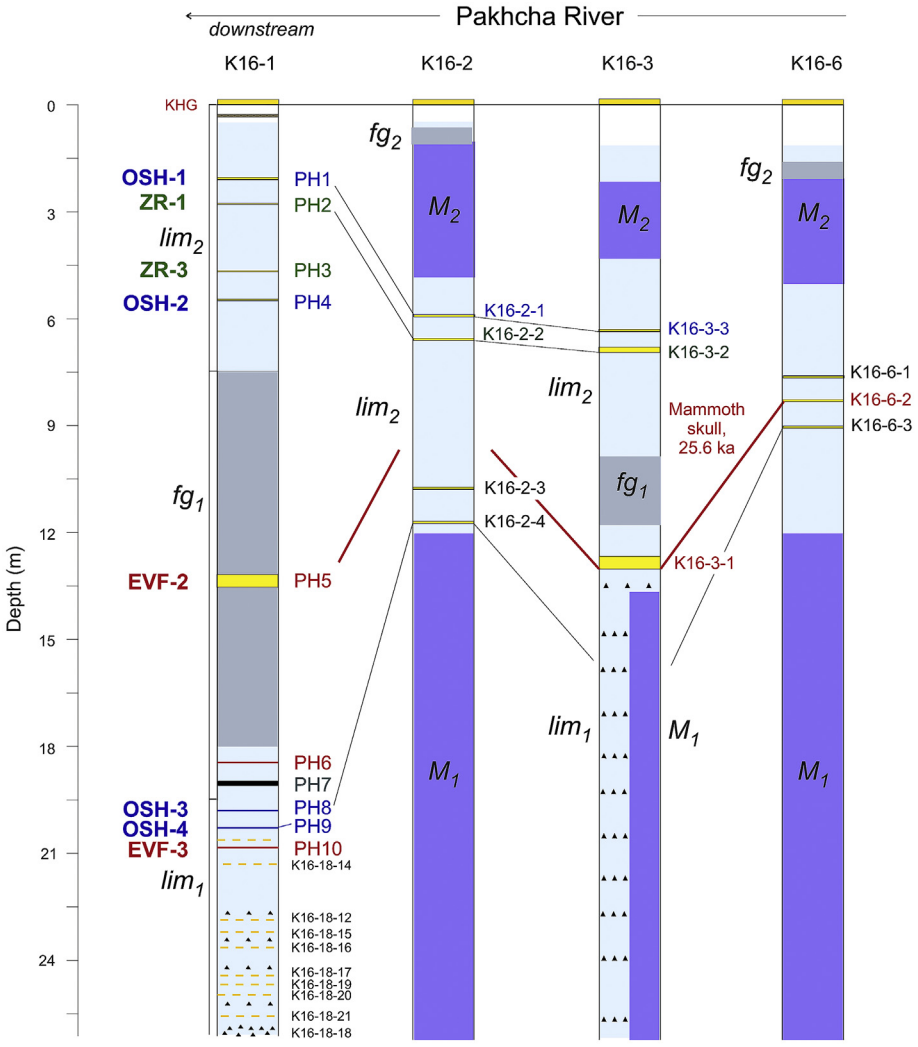

Fig. 4. Graphic representation of sections through the lacustrine and glacial deposits in the Pakhcha valley. Tephra labels as in Fig. 3. Deposits are labeled following Kraevaya and Kuralenko (1983): lim1 and lim2 - lacustrine deposits; fg_1 and M1 - glaciofluvial deposits and glacial till of stage I of the late Pleistocene glaciation, respectively; fg_2 and M2 - glaciofluvial deposits and glacial till of stage II of the late Pleistocene glaciation, respectively. Other captions as in Fig. 3.

data, and easy identification and rejection of analyses contaminated by mineral phases. Detailed description of the analytical setup, procedures of data quantification and quality control are provided by Portnyagin et al. (2020). The data for tephra glasses and reference materials obtained during the same analytical sessions are provided in Supplement 4.

For identification and correlation of tephras we compared our dataset to the database of glass compositions from the Kamchatka proximal pyroclastic deposits (Portnyagin et al., 2020); to available dataset for the submarine distal tephra from the NW Pacific (Derkachev et al., 2020); and to other analyses from our unpublished database.

Selected tephras from the proximitity of CKD volcanoes were studied under optical microscope to characterize their mineralogical assemblage and estimate semi-quantitative proportions of phenocrysts (Supplement 1). The mineralogical data were used for discrimination of tephras with very similar glass compositions originated from Shiveluch and Zarechny volcanoes, using previously published data on petrographic rock types from these volcanoes (Gorbach et al., 2013, 2018). To geochemically characterize lava from Kliuchi and Kozyrevsk we obtained three bulk rock analyses by X-ray fluorescence method in the Vinogradov Institute of Geochemistry SB RAS, Irkutsk, Russia, and compared those to the earlier published data (Supplement 5).

3.3. Chronology and stratigraphy

The age estimates for tephra layers are based on eleven AMS radiocarbon age measurements conducted at Beta Analytic Inc. (Miami): ten from the KamPlen section and one from the Kliuchi quarry (Table 1). All age measurements were performed on the organic fraction of bulk lacustrine sediments consisting primarily of pollen, spores, and organic residue from the abundant fossil diatom flora. The organic fraction was concentrated through sieving and mineral acid digestion. The ^{14}C dates were calibrated during age modeling using INTCAL13 curve (Reimer et al., 2013). The date for the pumice near Gorely volcano (source of one of the tephras in the study area) was obtained in the ^{14}CHRONO Center of Queen's University Belfast. An upper boundary for age modeling was set at the widespread KHG tephra from Khangar volcano, which was identified in Greenland and dated at 7872 ± 50 BP by Greenland Ice Core Chronology GICC05 (Cook et al., 2018). We report all radiocarbon ages as calendar ages (cal BP) or millennia (ka) before 1950 CE unless otherwise stated.

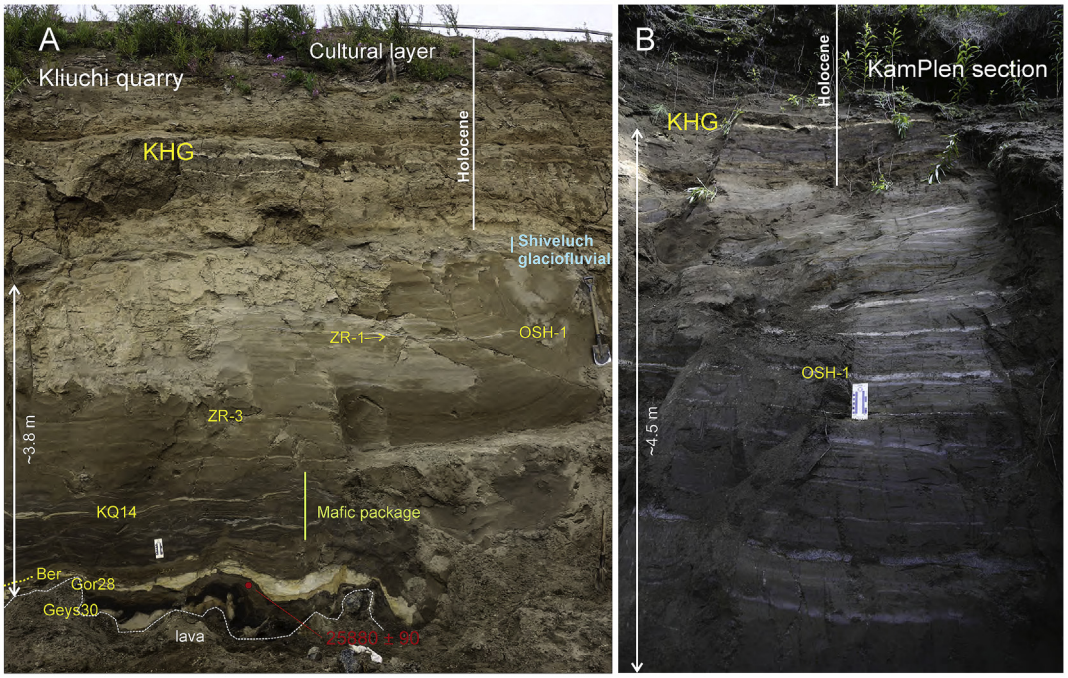

Fig. 5. Photos of key sections through the lacustrine deposits in the Kliuchi study area. **A.** Kliuchi quarry (site K18-8). Major marker tephras are labeled: KHG – marker tephra from Khangar volcano; *Ber, Gor28* and *Geys30* – marker tephra triad described in the text. Position of the radiocarbon sample and the obtained date are shown in red. Dark-brown and black layers at the bottom of the sequence are mafic cindery tephra. **B.** The upper part of the KamPlen section. Marker tephras are labeled as in Table 2 and Fig. 3. (For interpretation of the references to color in this figure legend, the reader is referred to the Web version of this article.)

To provide a comprehensive chronologic tool for the study, we constructed a reference Bayesian age-depth model for the KamPlen section based on eleven ^{14}C dates (Supplement 6). After major tephra layers were geochemically correlated among the key sections and to KamPlen, we were able to transfer their KamPlen age estimates to other studied sections and to model the ages of major tephras sandwiched between those dated in KamPlen (Fig. 7).

KamPlen age model was calculated in Bacon software following the approach of Blaauw and Christen (2011): sediments were considered as a sequence of small subsections with accumulation rate stochastically inherited from preceding subsections. The resulting age-depth model was averaged by many runs of Monte Carlo Markov chain of such subsections. Instantaneous ash-falls sharply differ from the continuously accumulating lake sediments, so we subtracted ash layers from model ("Slump" function in Bacon). The output of the modeling is a set of mean, median and 95% confidence range for ages of each centimeter in the section (Supplement 6). For the aims of this study, tephra ages were picked out of the dataset. Modeled tephra ages with 95% (2 sigma) error are provided in Table 2 and Supplement 1; in text and figures we use mean age values. On the basis of KamPlen age-depth model, we calculated a graph of accumulation rate probability versus age using Bacon package (Blaauw and Christen, 2011) (Fig. 8).

Upon the correlation of marker tephras from KamPlen to other sites, we were able to model the ages of marker tephras absent in KamPlen (Figs. 7 and 8). The studied sections, except for KamPlen, have few age references, which hampers accurate sedimentation rate modeling. These four sections (1–4 on Fig. 7) were modeled in OxCal software (Bronk Ramsey 2009). For Kharchinsky Lake (site K18-13) and Pakhcha (site K16-1) sections, we considered stratigraphical order with no assumptions on sedimentation rate and its variability. For Berezovy Yar (site 937), KamPlen reference model provided sufficient amount of age tie-points for rough extrapolation some 1.5 kyr below KamPlen model using Poisson sedimentation model (Bronk Ramsey 2008) with parameter *k* varying within two orders of magnitude (Bronk Ramsey and Lee 2013). The mean *k* from Berezovy Yar was utilized for Kliuchi Quarry (site K18-8), where only four age tie-points bracket undated tephra layer.

4. Results

4.1. Tephra sequences

4.1.1. General structure of the sections

All sections in the study area are topped with the Holocene soil-pyroclastic cover similar to that described by Braitseva et al. (1997) and Pevzner et al. (2006). The set of marker tephras partly varies between the northern and southern parts of our study area, but everywhere contains two major markers: KS_1 tephra from Ksudach volcano, and KHG from Khangar volcano. The cover is exclusively subaerial; its well-expressed layering is explained by alternating tephra and paleosol horizons. The overall color of the Holocene soil-pyroclastic sequence is brown with several light-colored tephra layers (Fig. 5A and B).

Contact of the Holocene cover with the underlying tephra-bearing lacustrine deposits is often sharp, with dramatic change of sediment color from brown to pale-gray (Fig. 5B). However, in most cases the contact is graded, without signs of an erosional discontinuity. Lacustrine deposits at different sites display a variety of structures, grain sizes, and textures largely dependent on proximity to the sediment source (Supplement 2, Figs. S2-S6). In the eastern part of the Kliuchi area, a layer of glaciofluvial deposits comprised of Shiveluch-sourced andesitic material, lies in the upper part of the lacustrine deposits and thickens to the east (Fig. 3 and Supplement 2, Fig. S7). On Shiveluch slope, glacial till and glaciofluvial deposits form a complex succession, which in places includes lenses of Shiveluch pumice or layers of fine ash.

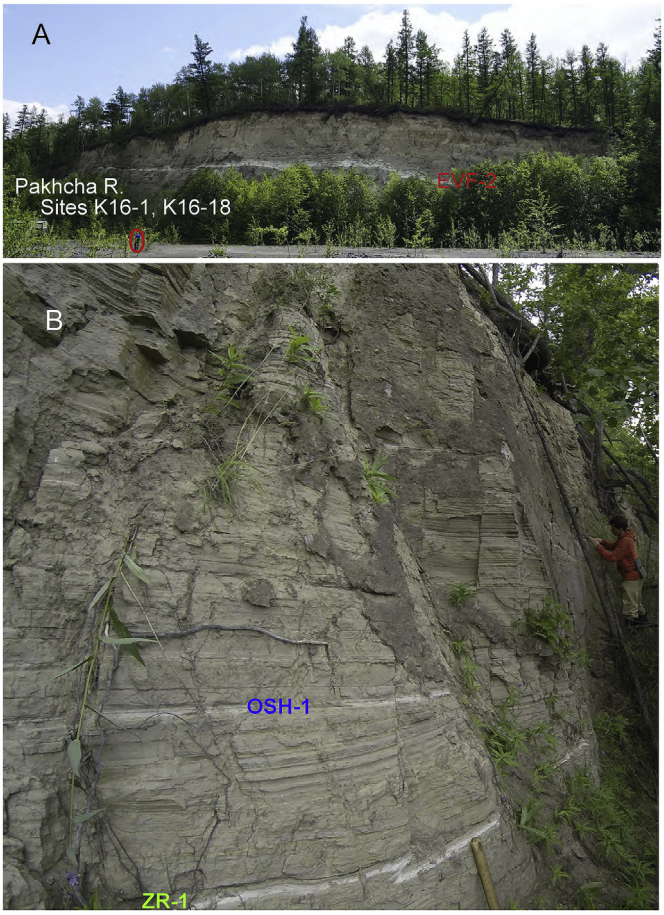

Fig. 6. General view (**A**) and detail (**B**) of the key outcrop in the Pakhcha valley (site K16-1 (K16-18)). Marker tephras are labeled as in Table 2 and Fig. 3. In **A**, a person in a red oval in the lower left part of the photo provides the scale. (For interpretation of the references to color in this figure legend, the reader is referred to the Web version of this article.)

4.1.2. Kliuchi area

Our major section, labeled KamPlen, was measured in a ~10 m-high natural outcrop at the Kliuchevskoe Lake shore (Figs. 2B and 3). It exhibits 7.5 m thick tephra-bearing lacustrine deposits (Fig. 5B and Supplement 2, Fig. S2) overlain by 2.8 m of Holocene subaerial soil-pyroclastic sequence (Figs. 2B and 5B). For this study, we measured KamPlen section for 8.5 m down from the KHG tephra dated at 7872 ± 50 BP in Greenland ice (Cook et al., 2018), obtained ten radiocarbon dates for this interval (Table 1), and sampled and analyzed 45 tephra layers (Fig. 3; Supplement 1). The second key site in this area is a quarry in Kliuchi town (site K18-8, Figs. 2B and 3), where we measured a similar section of lacustrine deposits (Fig. 5A and Supplement 2, Fig. S4) and obtained a radiocarbon date and geochemical data on 21 tephra samples. In addition, we examined eight shorter sections in the area, including a natural outcrop at the Kharchinsky Lake (sites K18-12 and −13), a road cut near Kliuchi pier (in different years labeled as K13-02, −20; and K15-8), a trench K13-04, and quarry sites 7582 and K18-7 (Fig. 2B and Supplement 2, Figs. S3 and S7). From these sections, we obtained geochemical data on 28 more tephra samples.

A prominent feature of the longest tephra sequences in the Kliuchi area (K18−8 and K13-20) is the presence of three brightly colored marker tephra layers at the very bottom of the outcrops (Figs. 5A and 9A). Distinct colors (from top to bottom: white, bright yellow, and pale-beige) make this tephra triad easily recognizable in the field. The lowermost tephra directly overlies mega-plagiophyric basaltic trachyandesite lavas from the regional fissure zone superimposed on the Plosky volcanic massif (Figs. 5A and 9A; Supplement 5; Flerov et al., 2017). Two more sections in the area feature only the two upper tephras from this group due to the incomplete excavation of the bottom sediments (Fig. 3). Another interesting feature of the Kliuchi area sections is the presence of a distinct package of dark-gray cindery tephra layers stratigraphically positioned above this marker tephra triad (Figs. 3 and 5A).

4.1.3. Kozyrevsk area

In the Kozyrevsk area, our key site (K16-1 aka K16-18) is a natural outcrop in the Pakhcha River valley, an artificially dammed channel of Studenaya River, now filled with water during spring snowmelt or heavy rainfalls but dry at other times (Figs. 1, 2B and 4, and 6). In this valley, Kraevaya (1977) and Kraevaya and Kuralenko (1983) described up to 32 m-high outcrops, which exhibit packages of lacustrine sediments interlayered with two glacial tills and related glaciofluvial deposits. These outcrops are located only 25−35 km away from the Tolbachik and Ushkovsky volcanic massifs and at similar distance from the terminal parts of modern glaciers (Fig. 1). The 27 m high outcrop on the left bank of the valley (key site K16-1 aka K16-18) contains two lacustrine packages (lower, 5 m thick “lim1” and upper, 7 m thick “lim2”, labeled according to Kraevaya and Kuralenko, 1983) separated by a 13 m thick glaciofluvial package (fg1) (Figs. 4 and 6). We analyzed 22 tephra samples from both lacustrine and glaciofluvial deposits; the most prominent of them is a snow-white partly reworked fine ash in the middle of the glaciofluvial package fg1 (Fig. 6A).

The other sampled sections in the Pakhcha valley are located along its right bank, 1, 2.6, and 5.6 km upstream from site K16-1 (Figs. 2C and 4). The first one (K16-2) exposes two glacial tills

Table 1
Radiocarbon age measurements and associated calendar age ranges calculated as highest probability density (HPD) at 95% (Bronk Ramsey, 2009).

Location	Sample name	Lab ID	Depth (cm)	Material	Radiocarbon age (yrs BP)	95% HPD range (cal yrs BP)
Kliuchevskoe Lake	KamPlen 101	Beta-478709	101	organo-mineral sediment	9990 ± 30	11613−11285
“-“	KamPlen 175	Beta-539402	175	organo-mineral sediment	12150 ± 40	14120−13960
“-“	KamPlen 267	Beta-478707	267	organo-mineral sediment	14300 ± 40	17595−17229
“-“	KamPlen 336	Beta-478708	336	organo-mineral sediment	15440 ± 40	18810−18590
“-“	KamPlen 447	Beta-433775	447	organo-mineral sediment	17530 ± 60	21360−20995
“-“	KamPlen 591	Beta-478705	591	organo-mineral sediment	19090 ± 50	23273−22772
“-“	KamPlen 655	Beta-478706	655	organo-mineral sediment	20060 ± 60	24336−23912
“-“	KamPlen 802	Beta-432011	802	organo-mineral sediment	24010 ± 100	28255−27835
“-“	KamPlen 823	Beta-405620	823	organo-mineral sediment	24420 ± 90	28655−28295
“-“	KamPlen 835	Beta-471112	835	organo-mineral sediment	23710 ± 80	27954−27622
Kliuchi quarry	K18-8-A	Beta-529664	–	organo-mineral sediment	25880 ± 90	30522−29702
Mutnovsky volcano, Opasny Canyon	K12-02-6	UBA-23700	–	organo-mineral sediment	29841 ± 234	33566−34386

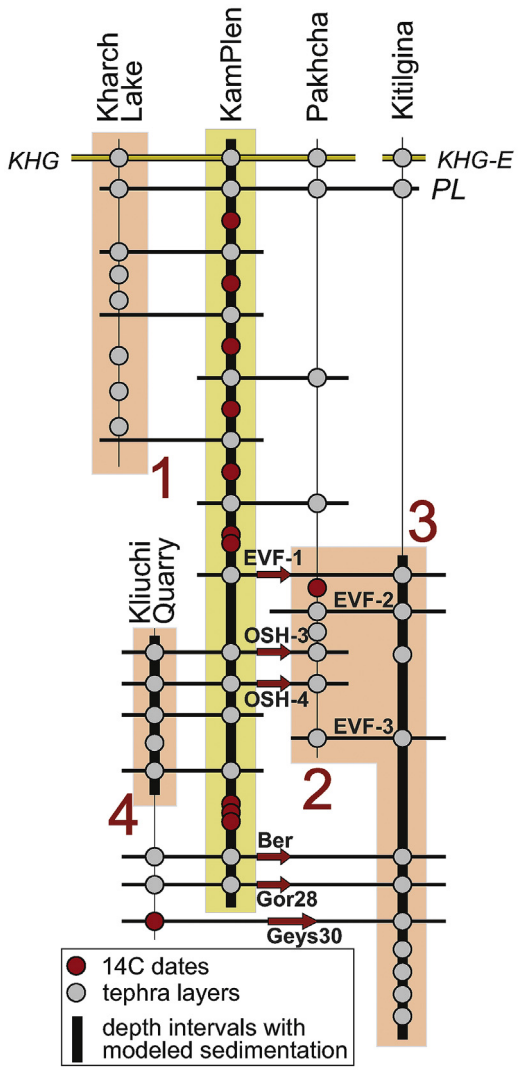

Fig. 7. A schematic representation of age models for late Pleistocene sedimentary records in the Central Kamchatka Depression. Individual sections are labeled, gold background is for Bacon age-depth model, red background - for OxCal Sequence (1, 2) and P_Sequence (3, 4) models. The age models go down from Khangar tephra (KHG) dated by Greenland Ice Core Chronology (GICC05) (Cook et al., 2018). KHG-E – another Khangar tephra close in time to KHG (Zelenin et al., 2020). Other tephra labels as in Figs. 3 and 8. Arrows indicate dates transferred to the Pakhcha-Kitilgina age model. See text for additional explanations. (For interpretation of the references to color in this figure legend, the reader is referred to the Web version of this article.)

(M1 and M2 in Kraevaya and Kuralenko, 1983) separated by a tephra-bearing lacustrine package (Fig. 4 and Supplement 2, Fig. S8), the next one (K16-3) exposes a complex combination of glacial till (M1), glaciofluvial and lacustrine deposits (Fig. 4 and Supplement 2, Fig. S9), and the uppermost one exposes two tills separated with 0.5–2 m thick thinly stratified lacustrine deposits. We sampled ten major tephra layers from these outcrops in order to correlate those to K16-1 (Fig. 4). In addition, we sampled a tephra layer from a lacustrine package positioned between the Holocene sequence and the lower glacial till (M1) in the main channel of the Studenaia River, 3.5 km south of K16-1 (Fig. 2C). Kraevaya and Kuralenko (1983) reported a finding of a mammoth skull within the lacustrine deposits lim2, with three ^{14}C dates from the skull yielding an average age of ~25.6 ka BP after calibration with IntCal13.

In addition, in the Kozyrevsk area we examined tephras in the upper part of the lacustrine sediments in Kozyrevsk town (sites K15–22 and K18-2), Ushki archaeological excavation (site K9–U5) (Dikov, 2003; Goebel et al., 2003; Goebel et al., 2010) and at the Sredinny Range slope across the Kamchatka river from Kozyrevsk (site K18-6) (Fig. 2C).

4.1.4. Kitilgina River

A key site in the Kitilgina River valley is Berezovy Yar (site 937), ~120 km south of the Kozyrevsk area. This 15 m-high natural bluff exhibits seventeen tephra layers buried within lacustrine deposits, which overlies a 0.3 m thick layer of laminar sand underlain by a 3-m thick matrix-rich gravel layer (Figs. 1 and 9B; Supplement 2, Fig. S5). Fifteen tephras are light- or (rarely) dark-colored pumiceous ash and two are dark-gray cindery ash. The most prominent layers are a white thick ash in the middle of the section and three closely spaced tephra layers close to its bottom (Figs. 3 and 9B). In addition, we sampled two light-colored tephra layers in the outcrop at the Kamchatka River bank (site K16-8), 15 km WNW from the Kitilgina site.

4.2. Tephra composition and correlations

4.2.1. Two major groups of tephra

Examination of tephra samples under optical microscope and by back-scattered electron imaging has allowed us to identify two groups of tephras: (1) dominantly vitric distal ash with inflated highly vesicular glass shards, and (2) crystal-rich ash likely from local volcanoes (Fig. 10). Tephras from these two groups also differ in appearance: those from the first “distal” group are white, tan or bright yellow, while most of the "local" tephras are dull-gray to black, and a few are white with black speckles (“salt-and-pepper” color). Vitric tephras dominate the southernmost sites while the majority of mineral-laden tephras are found in the KamPlen and other northern sites. On the geochemical bi-plots glass from most of the vitric tephras form tight clusters or trends in the rhyolitic field (Fig. 11). The majority of these glasses fall into either high-K or medium-to-low-K fields. Mineral-rich tephras also contain mostly rhyolitic glass with some basaltic to andesitic glass in cinders. These glasses fall mainly in the medium- or high-K compositional fields.

4.2.2. Major marker layers

Correlations of tephra layers between sections were constrained by their stratigraphic positions (Figs. 3, 4 and 8) and geochemical compositions of glass (Figs. 12–14). Table 2 shows major marker layers, which provide correlations between the study areas. In addition, it includes several potential tephra markers, which were found in only one section/study area but based on their composition and dominance of vitric glass shards may serve as distal markers once more sections are described in adjacent areas. Major tephras occurring in two and more areas were assigned individual codes (Figs. 3, 4 and 8; Table 2).

A remarkable triad of silicic marker tephras found at the bottom of the northern Kliuchi sections K18–8 and K13-20 correlates to three prominent tephra layers positioned close to the bottom of the southernmost site 937 in Kitilgina area (Figs. 1, 3 and 8). In addition, in Kliuchi area, the upper two of these tephras were found also in KamPlen, where springs prevented a deeper excavation, and in section K13-04 (Fig. 2B). In Pakhcha (section K16-18), glass shards from these three tephras are scattered through the lowermost 2.5 m of the sediments with no well-expressed peaks of each tephra and a large admixture of compositionally different glasses (Figs. 8, 9C and 12A). This suggests reworking of these tephras in the fast accumulating sediments rich in reworked cinder particles; the original fallout layers may be somewhat lower in the covered part of the sediments, which is supported by correlation of

Table 2
Major distal marker tephra layers in the late Pleistocene deposits in the Central Kamchatka depression.

Tephra ID	Source zone	Source volcano	Age - min (mean) max (cal BP)	Glass composition/Mineralogy	Tephra IDs in individual sections		
					Kliuchi area	Kozyrevsk area	Kitilgina R.
SH #61a	CKD	Shiveluch	11572 (11984) 12517	Med- to high-K/Pl > Hbl ± Px	KamPlen1, KP1, KH1	U1	–
SVK-1	SR	?	14041 (14401) 14915	High-K rhyolite/vitric	KamPlen6, KQ2?	SR1	–
OSH-1	CKD	Shiveluch	18464 (18648) 18807	Med-K rhyolite/Pl > Hbl ± Px	KamPlen20, KQ7	PH1	–
ZR-1	CKD	Zarechny	18970 (19324) 19738	Med-K rhyolite/ Hbl > Cpx + Opx ± Ol > Pl	KamPlen25, KQ8	PH2	BY1
ZR-2	CKD	Zarechny	19257 (19679) 20132	Med-K rhyolite/ Hbl > Cpx + Opx ± Ol > Pl	KamPlen26		BY2
SVK-2	SR	?	20591 (20984) 21244	High-K rhyolite/vitric	KamPlen31	-	-
ZR-3	CKD	Zarechny	20980 (21384) 21730	Med-K rhyolite/ Hbl > Cpx + Opx ± Ol > Pl	KamPlen33, KQ10?	PH3	–
OSH-2	CKD	Shiveluch	21177 (21591) 21965	Med-K rhyolite/Pl > Hbl ± Px	KamPlen34	PH4	–
KamPlen36	VF	?	24008 (24281) 24794	Low- to med-K rhyolitic trend/vitric	KamPlen36	-	-
EVF-1	VF	?	24729 (25288) 25917	Low- to med-K rhyolite/vitric	KamPlen37	–	BY3
EVF-2	VF	?	25481 (25785) 26089*	Low- to med-K rhyolitic trend/vitric	–	PH5	BY4
PH6	VF	?	25608 (25963) 26339*	Low- to med-K rhyolite/vitric	–	PH6	-
OSH-3	CKD	Shiveluch	25519 (26153) 26770	Med-K rhyolite/Pl > Hbl ± Px	KamPlen38, KP2	PH8	–
OSH-4	CKD	Shiveluch	25918 (26322) 26734	Med-K rhyolite/Pl > Hbl ± Px	KamPlen40, KP3, KQ12	PH9	–
BY5	SR	?	25732 (26362) 27053	High-K rhyolite/vitric	–	–	BY5
EVF-3	VF	?	25985 (26488) 26930*	Low- to med-K rhyolitic trend/vitric	–	PH10	BY6
KQ14	VF	?	26743 (27343) 27906*	Low-K rhyolite/vitric	KQ14	-	-
Ber	SR	Spokoiny volcano area	27768 (28204) 28494	High-K rhyolite/vitric	KamPlen43, KP5, KQ18	–	BY8
Gor28	RA	Gorely	27856 (28316) 28623	High-K rhyolite/vitric	KamPlen44, KP6, KQ19	–	BY9
BY10	?	?	28126 (28739) 29881*	Low-K dacitic trend/Mineral-rich	-	-	BY10
Geys30	VF	Geysernaya	29533 (29949) 30385*	Low- to med-K rhyolitic trend/vitric	KP8, KQ21	–	BY11
BY13	CKD	Bolshaya Udina	29530 (30031) 30567*	Med-K rhyolitic trend/mineral-rich	-	-	BY13
BY14	VF	?	29536 (30083) 30698*	Low- to med-K rhyolite/vitric	-	-	BY14
BY15	VF	Karymsky volcanic center	29540 (30123) 30800*	Med-K dacite/vitric	-	-	BY15
BY16	SR	?	29560 (30174) 30917*	High-K rhyolite/vitric	-	-	BY16

Note: The table includes major marker tephra layers identified in the study area. Modeled tephra ages are given with 95% (2 sigma) error. Most of age estimates are based on the KamPlen age-depth model. Ages marked with an asterisk are calculated within local models and thus have larger error.

reworked cinders to those from the Kliuchi cindery package (Fig. 3).

Comparison of the glass composition from these three major marker tephras to our TephraKam database of glasses from proximal Kamchatka pyroclastic deposits (Portnyagin et al., 2020) permits their following identification.

The lowermost tephra in the triad (*Geys30*) contains glass of medium-K rhyolite composition close to the boundary between the medium- and low-K fields (Fig. 12A). The relatively K_2O-poor composition as well as low Nb/Y and La/Y ratios (Fig. 13) testify the VF provenance. The major and trace elements in this tephra match closely the composition of pumice lapilli presumably originated from the Geysernaya caldera (Figs. 1, 12A and 14A). This tephra is fine to medium-sand in Kliuchi and coarse ash with pumice lapilli up to 2.5 cm in Kitilgina area (Fig. 9A and B). The spatial variations of the grain size are also consistent with the identification of the Geysernaya caldera as the tephra source (Fig. 1). Geysernaya tephra may be an important marker for the region based on its wide dispersal and thickness, including in the most northern sites (Supplement 1; Fig. 1). Based on our age model, this tephra has an age of ~30 ka, and therefore it was labeled as *Geys30* (Table 2). The *Geys30* tephra provides an age estimate for the bottom of the Kliuchi sections and for the underlying lava (Figs. 3, 8 and 9A).

The middle tephra of the marker triad (*Gor28*) has matrix glass of high-K relatively low-SiO_2 (~70 wt%) composition that together with elevated Nb/Y (~0.26) and moderately high La/Y (~0.6) points to its origin from a rear-arc volcano (Figs. 12A and 13). The tephra geochemically matches pumice from the Gorely eruptive center in the South Kamchatka rear-arc (Portnyagin et al., 2020), and was likely derived from its most recent caldera-forming eruption ("dacite pumice" in Selyangin and Ponomareva, 1999) (Figs. 12A and 14B). Distal tephra from this eruption was earlier reported north and east from the caldera: from the city of Petropavlovsk-Kamchatsky (Melekestsev et al., 1992) and from marine core SO201-2-40 on the Meiji Seamount (Derkachev et al., 2020) (Fig. 1). Based on bulk composition, a Gorely origin was also suggested for a distal tephra found in the Ledovy Bluff outcrop in Chukotka, ~1600 km NNE from the source (Fig. 1, inset; Melekestsev et al., 1991a). Our data for this distal ash (Figs. 12A and 14B, Supplements 3 and 4) confirm this identification. In addition, our geochemical data on a tephra from the marine core ODP145-883D described by Bigg et al. (2008) ~700 km SSE of the Gorely also suggests derivation from this volcano (Figs. 12A and 14B; Supplements 3 and 4). Terrestrial Gorely tephra sites suggest dominantly northern dispersal of this tephra (Fig. 1, inset), while two marine sites point to an eastern dispersal. Glass compositions from the northern and eastern lobes are identical (Figs. 12A and 14B).

Our age estimate for *Gor28* tephra according to the KamPlen age-depth model is 28.3 ka (Table 2). In addition, the date under *Gor28* tephra obtained in the Kliuchi quarry (Table 1, Figs. 3 and 9A) also suggests that this tephra is younger than ~30 ka. Published age estimates for this tephra vary between ~37.8 (36168–39515) north and ~39.4 or ~39 ka east of the caldera (Melekestsev et al., 1992; Bigg et al., 2008; Derkachev et al., 2020). The first age estimate was obtained on a thick organic-poor paleosol underlying the tephra so it is likely somewhat older than the ash deposition. Marine age estimates have unspecified errors, which might reach ±5 ka

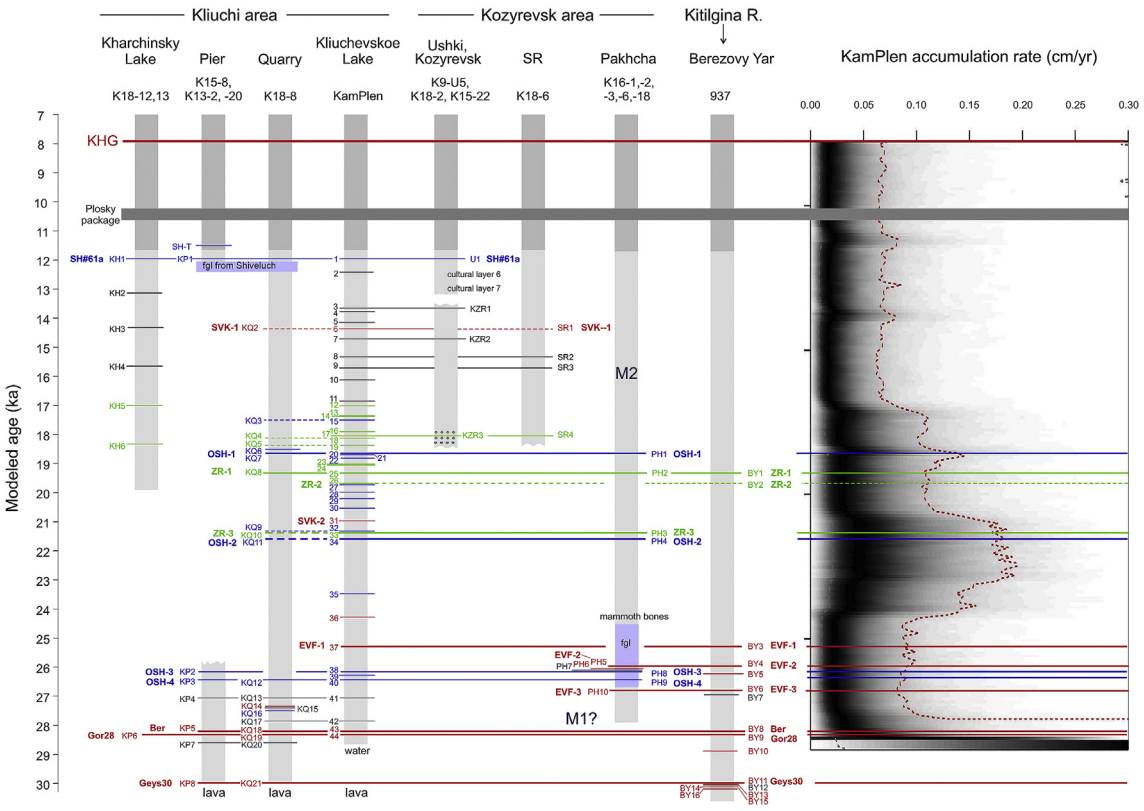

Fig. 8. Tephrochronological model for the late Pleistocene tephras in the CKD (**A**) and their position relative to changes in the accumulation rate for the KamPlen sediments (**B**). Tephras are color coded and labeled as in Fig. 3 and Table 2 and Supplement 1. (For interpretation of the references to color in this figure legend, the reader is referred to the Web version of this article.)

(Derkachev et al., 2020). In Chukotka, the Gorely tephra age was roughly estimated at ~42 (40418–43762) ka (calibrated from the original ^{14}C date of 38000 ± 1000; Kotov et al., 1989). However, the tephra layer was found only in one part of the outcrop and its exact position relative to the dated level remains unclear (Kotov et al., 1989; Melekestsev et al., 1991a).

To resolve the discrepancy between the available age estimates we attempted to date the proximal pumice of this eruption. The only site where we were able to find some organic matter suitable for dating was located east of the Gorely caldera, i.e. in the direction towards marine cores. The organic material was extracted from a silt layer not immediately from under this tephra but ~130 cm below it, from under an underlying and compositionally different pumice unit. The obtained date (Table 1) suggests that the Gorely tephra was deposited sometime later than ~33.9 ka, which is closer to our age estimate of 28.3 ka rather than to ~40 ka estimate from the marine cores. The reasons for such a large array of age estimates need further investigation and may suggest two compositionally similar but separate Gorely eruptions: the 28 ka tephra went to the north and the ~40 ka tephra – to the east, towards cores SO201-2-40 and ODP145-883 (Fig. 1, inset). However, our proximal date was obtained east of the volcano. Therefore, if an earlier eruption occurred, the deposits of that event must have been eroded from this section.

The upper tephra in the marker triad (*Ber*) is a white ash with high-K and high-Nb composition (Figs. 12A and 13), which suggests eruption from a SR volcano (Portnyagin et al., 2020). The source volcano of this tephra cannot be precisely identified using the presently available data. In the TephraKam database (Portnyagin et al., 2020), the *Ber* composition is close to sample of welded tuff #487-5 sourced from the Spokoiny volcano area in SR (Figs. 1, 2A and 14C). In comparison with this sample, *Ber* glass has higher Sr and Eu contents and can be produced by smaller degree of fractionation than #487–5, but originate from the same source. Rhyolite glasses from Khangar volcano (e.g., Cook et al., 2018) are also similar to *Ber*, but they have systematically lower Pb/Ce and Cs/Rb ratios.

The *Ber* tephra thickness is greater in the southernmost Kitilgina area (site 937), while the grain size is larger in Kliuchi (Supplement 1). The age estimate for this tephra is ~28.2 ka in KamPlen section (Table 2). Search in our database has allowed us to identify a visible layer of compositionally identical ash in cores SO201-2-114 (Bering Sea) and SO201-2-9-pilot (Pacific Ocean), and similar glass in a sediment layer in core SO201-2-85 (Bering Sea) (Fig. 1, inset; Dullo et al., 2009; for depths of submarine tephras see Supplement 3). In core SO201-2-85, these glasses are spread in the interval corresponding to ~42–46 ka (Riethdorf et al., 2013), which is 14–18 ka older than our estimate. This discrepancy resembles Gorely case and can be resolved when more dates for this tephra are available. Based on its wide dispersal, this tephra, which we labeled *Ber*, also can serve as a marker for the terrestrial and marine late Pleistocene deposits.

Four other vitric tephra markers provide more correlations between at least two of the study areas (Table 2; Figs. 8, 12B and 14D-F).

(1) *SVK-1* tephra links Kliuchi and Kozyrevsk areas, however, in both areas it is < 1 cm-thick suggesting either a medium-size eruption or an eruption from a distant source. This tephra is characterized by high-K and high-Nb glass composition

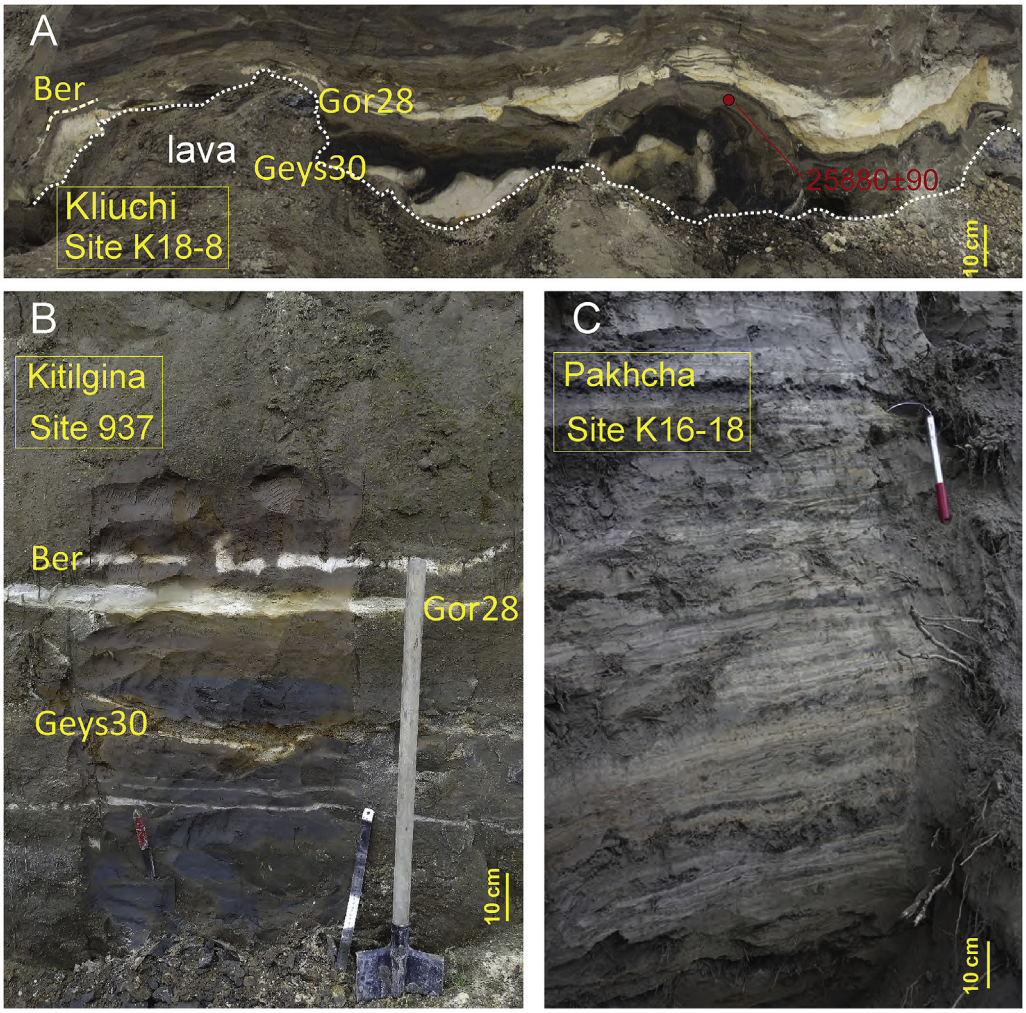

Fig. 9. Bottoms of the key sections in Kliuchi (**A**), Kitilgina (**B**), and Pakhcha (**C**) study areas. Major marker tephras are labeled as in Table 2 and Figs. 3 and 8. In **A:** position of the radiocarbon date is shown in red; black layer above *Geys30* ash is cindery tephra. (For interpretation of the references to color in this figure legend, the reader is referred to the Web version of this article.)

typical for Sredinny Range volcanoes (Figs. 12B and 13) and strikingly resembling tephra from the Holocene Svetly Kliuch crater on the eastern slope of the Sredinny Range (Fig. 1) as well as some of the Holocene eruptives from Ichinsky volcano (Fig. 14D; Pevzner, 2015; Portnyagin et al., 2020). Based on this resemblance, we provisionally assign it to either one of the late Pleistocene monogenetic vents located in the Svetly Kliuch area (Fig. 1; Ogorodov et al., 1972) or to Ichinsky. Based on the age model for KamPlen this tephra was deposited ~14.4 ka BP.

(2) *EVF-1* tephra links Kliuchi area with Kitilgina sites (Fig. 8). It is thicker (2 cm) in Kitilgina than in KamPlen (1 cm). Based on its rhyolitic and relatively K_2O-poor composition close to the boundary between low- and medium-K fields (Fig. 12B), and low Nb/Y and La/Y similar to *Geys30* tephra (Fig. 13E), it was derived from a frontal volcano (Volynets et al., 1994; Portnyagin et al., 2020). *EVF-1* is compositionally similar to the Kuril Lake tephra (KO), particularly for highly incompatible trace elements in the left part of the normalized patterns (Fig. 14E). Its modeled age is ~25.3 ka (Table 2).

(3) *EVF-2* tephra links Kozyrevsk area (Pakhcha) to Kitilgina. This is the most prominent tephra in Pakhcha and Kitilgina valleys (Figs. 3, 4 and 6A). Its original thickness in Pakhcha is likely 10–15 cm. In Kitilgina area it varies from 4 to 40 cm and is ~10 cm on average. Glass from *EVF-2* tephra forms a trend in the rhyolitic field from 73 to 77 wt% SiO_2 close to the boundary between low- and medium-K compositions (Fig. 12B). This compositional feature as well as low Nb/Y (Fig. 13) suggest derivation of this tephra from a source in the volcanic front (Volynets et al., 1994; Portnyagin et al., 2020). In most major and trace elements this tephra is similar to the Geysernaya caldera glasses (Figs. 1, 12 and 134F), but has larger range of SiO_2 and lower MgO and TiO_2 in comparison with the latter. The most SiO_2-rich glasses from *EVF-2* tephra have similar major element compositions with WP2 tephra in core SO201-2-40 on Meiji Seamount (Derkachev et al., 2020) (Figs. 1 and 14F). Average trace element compositions of these tephras are slightly different, but the difference is statistically insignificant. The age estimate for WP2 tephra (~28 ka) (Derkachev et al., 2020) is close to our estimate of ~26 ka (Table 2). Thus, WP2 tephra can be likely a distal analog of the EVF-2 tephra.

(4) *EVF-3* also links Kozyrevsk area (Pakhcha) to Kitilgina. This tephra is compositionally very close to the previous one falling into the low-Si part of the *EVF-2* trend (Figs. 12B, 13 and 14F), which very likely suggests the same source in the

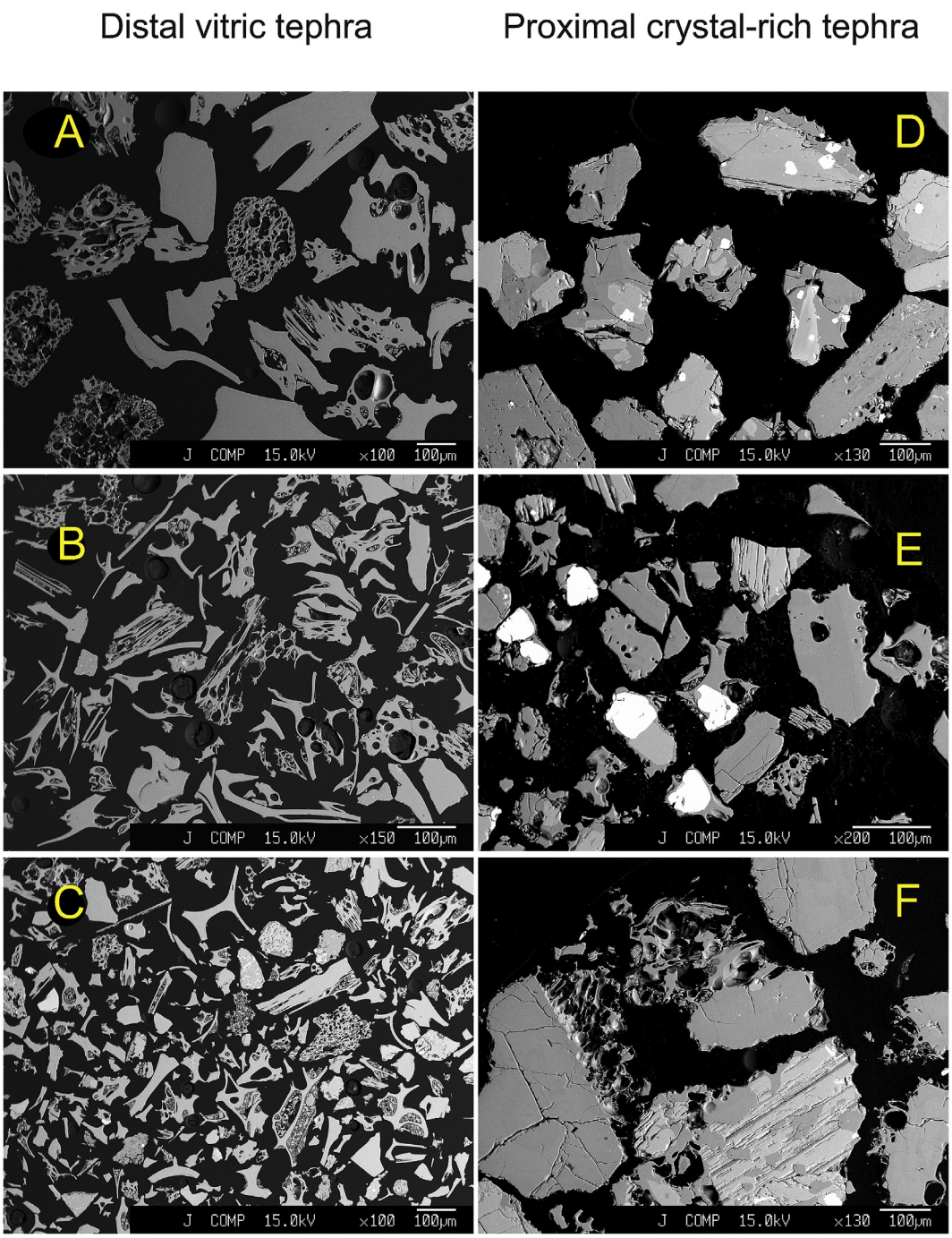

Fig. 10. Back-scattered electron images of representative tephras. Left column, distal vitric tephra: **A** – *Ber* (sample K18-8-29), **B** – *Gor28* (K18-8-30), **C**- *Geys30* (K18-8-33). Right column, typical crystal-rich local tephra in the northern part of the study area: **D** – Baidarny, **E** – Zarechny, **F** – Shiveluch.

volcanic front. However, it is only 2 cm thick in both areas, which may suggest a smaller eruption or a different ash fall axis. Its modeled age is ~26.5 ka (Table 2). Based on close age estimates and very close trace element composition it might be an alternative correlative for distal WP2 tephra, but in our study area it has significantly lower SiO_2 contents (Fig. 12B).

4.2.3. Potential distal tephra markers

Several vitric tephras occur only in one of the study areas. However, based on their appearance and geochemical characteristics, they might occur in other areas as well. In Kliuchi area, these are the high-K *SVK-2* tephra compositionally close to *SVK-1,* but exhibiting a larger range of SiO_2 contents from 75 to 78 wt%, and the low-K *KQ14* tephra, likely derived from the volcanic front and very close to the Ksudach caldera products (Figs. 1, 1 and 32B, 13, 14D and G). *KamPlen36* layer has mixed composition: in addition to a scatter of background medium-K local glasses (Supplement 3) it contains rhyolitic glass shards forming a trend close to the boundary between low to medium-K fields (Fig. 12B, Table 2), which likely represent a distal tephra and be useful as a marker once more sections are measured in the area. In Kozyrevsk area

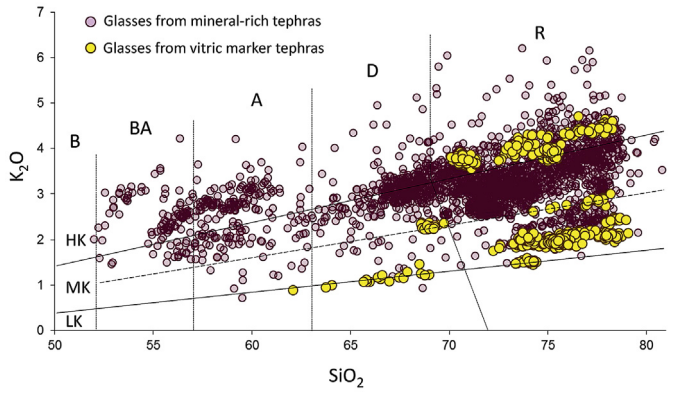

Fig. 11. Composition of volcanic glass from all the analyzed tephra samples. Glasses from vitric marker tephras are shown in yellow; glasses from mineral-rich tephras are in brown. Solid lines divide fields of low-K_2O (LK), medium-K_2O (MK), and high-K_2O (HK) basalts (B), basaltic andesites (BA), andesites (A), dacites (D), and rhyolites (R) at Na_2O = 5 wt% following Le Maitre et al. (2002). Dashed line divides the field of medium-K compositions into the upper and lower ranges for more convenient description of glass compositions. Oxide concentrations are given in wt%. (For interpretation of the references to color in this figure legend, the reader is referred to the Web version of this article.)

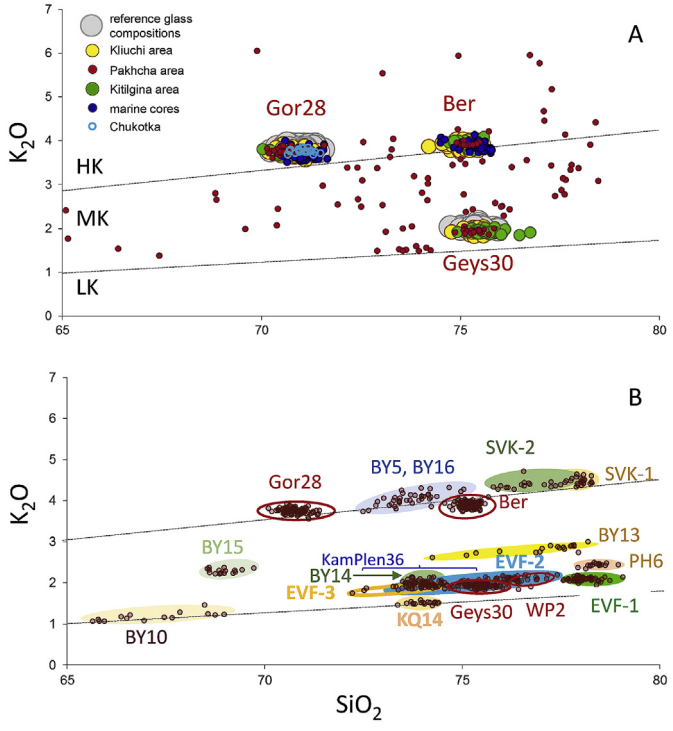

Fig. 12. Composition of glass from marker tephra. **A.** Composition of volcanic glass from the major marker tephra triad *(Ber, Gor28,* and *Geys30)* sampled in different study areas against reference compositions for proximal Gorely and Geysernaya pumice (Portnyagin et al., 2020). Red dots show mixed glass from the bottom of the Pakhcha section K18-16 with distinct populations of glasses from *Ber, Gor28,* and *Geys30* tephras. Dark-blue circles show *Ber* and *Gor28* glasses in the Bering Sea and Pacific cores (Derkachev et al., 2020; and unpublished authors' data). Turquoise circles show glass from *Gor28* tephra in the Ledovy Bluff (Chukotka). **B.** Composition of volcanic glass from all marker tephras (dark-brown transparent small circles). Glasses from individual tephras are shown with colored shading with matching tephra labels. Glasses from the marker tephra triad (*Ber, Gor28,* and *Geys30*) and WP2 from core SO201-2-40 (Derkachev et al., 2020) are shown with red ovals. Solid lines divide fields of low-K_2O (LK), medium-K_2O (MK), and high-K_2O (HK) glasses following Le Maitre et al. (2002). Oxide concentrations are given in wt%. . (For interpretation of the references to color in this figure legend, the reader is referred to the Web version of this article.)

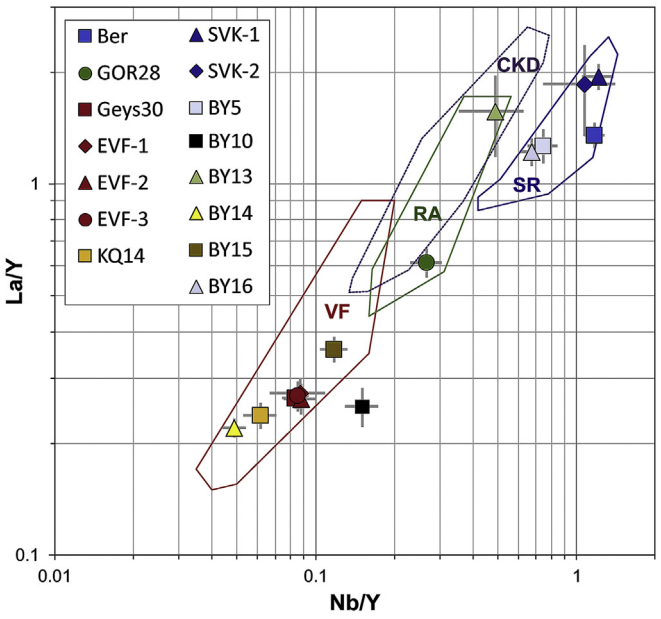

Fig. 13. Nb/Y–La/Y discrimination diagram for glass from marker tephras. Fields of different volcanic zones are after Portnyagin et al. (2020). VF – volcanic front, RA – rear-arc, CKD – Central Kamchatka Depression, SR – Sredinny Range. Error bars are 2 standard deviation of the mean ratios. Tephra codes correspond to those in Table 2 and Figs. 3 and 8.

(Pakhcha valley), tephra *PH-6* is also close to the same trend, however, it lies distinctly lower in the section sandwiched between *EVF-2* and *OSH-3* marker tephras (Figs. 8 and 12B).

In Kitilgina area, two potential marker tephras, *BY5* and *BY10*, are sandwiched between *EVF-2* and *EVF-3,* and Gor28 and Geys30, respectively. The rest four tephras, *BY13-BY16*, are stratigraphically positioned below *Geys30* tephra, so they have not been found in other sections as all of those feature only younger deposits. Tephras *BY5* and *BY16* have very similar compositions and based on their high-K and high-Nb/Y values originate from same source in the Sredinny Range (Figs. 12B and 13). In many trace elements the *BY5* and *BY16* glasses are similar to Khangar tephras but have higher Ti, Zr and Hf, as well as concentrations of the most incompatible elements (e.g., B, Cs, Rb) (Fig. 14H), so their source remains unclear. *BY10* layer is characterized by low-K glass similar to tephra from Ksudach volcano (Fig. 12B). However, this sample has distinctively high Nb/La and low Th/La in comparison with known Ksudach tephras, as well as all other tephras from Kamchatka (Figs. 13 and 14G). Thus, *BY10* has an exotic composition and could have been derived from another arc.

Tephra *BY13* has medium-K composition and relatively high Nb/Y and La/Y ratios suggesting volcanic source in the Central Kamchatka Depression (Fig. 13). In the TephraKam database (Portnyagin et al., 2020), the closest analog of *BY13* is a proximal pumice from the Bolshaya Udina volcano (Fig. 14I). Tephra *BY14* forms a cluster in a densely populated low-to medium-K field. Glass in tephra *BY15* has dacitic medium-K compositions. Both *BY14* and *BY15* have relatively low Nb/Y and were likely derived from the volcanic front (Figs. 12B and 13). *BY14* exhibits some similarity with *EVF-1* tephra, and may originate from the same source (Fig. 13E). *BY15* has similar concentrations of immobile major and trace elements to the samples #158–35 and #200–75 of welded tuffs from the middle Pleistocene Stena-Sobolinaya caldera (Fig. 13J). Variable enrichment of the welded tuffs in Rb, K and Li is a typical alteration feature (Portnyagin et al., 2020). Thus, *BY15* could originate from a younger eruption in the Karymsky volcanic center, comprising a

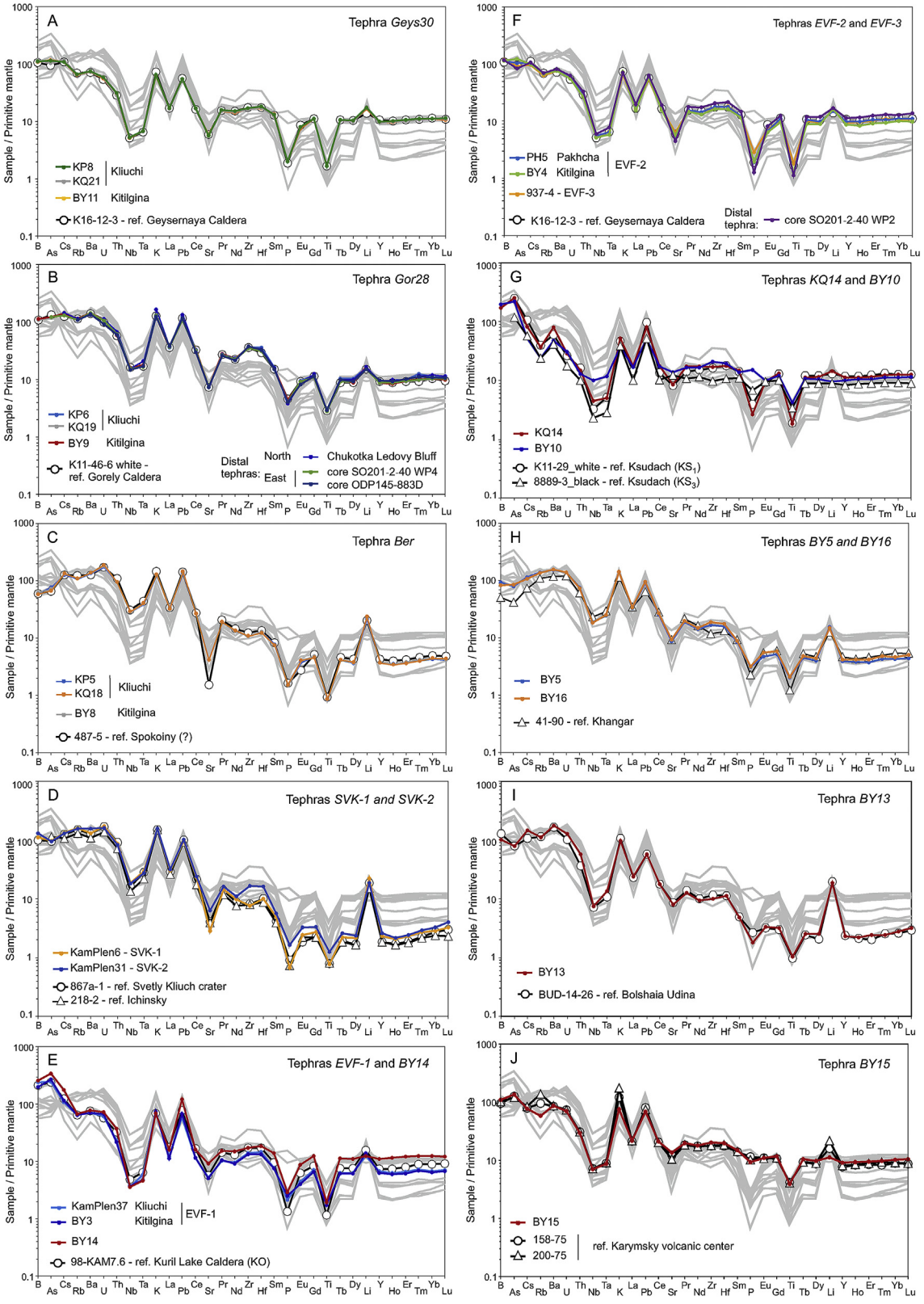

Fig. 14. Normalized trace element compositions of volcanic glass from marker tephras. Data on reference proximal samples of pumices and welded tuffs from Kamchatka from TephraKam database (Portnyagin et al., 2020) is marked with ref. symbol. WP2 glass composition is after Derkachev et al. (2020). Normalization to the bulk silicate Earth composition after McDonough and Sun (1995). Light gray patterns in the background are average compositions of all marker tephras from the study area.

number of nested calderas, including Stena-Sobolinaya caldera. One more vitric tephra, *K15-19*, was found within the eroded lacustrine deposits only 2–3 km away from major Pakhcha sites (Fig. 2C). It is very close in most of the major elements to *EVF-2*, but has higher TiO_2 and MgO contents so might represent an individual tephra not found in any other Pakhcha site.

4.2.4. Local tephra

Mineral-rich tephras occur mostly in the northern part of the study area and predominate in the KamPlen section (Figs. 3 and 5B). These tephras likely have a local provenance and they belong to two main groups: (1) black or dark-gray cinders with glasses ranging from 51 to 63% SiO_2, and (2) grayish or salt-and-pepper-colored sandy tephras with glasses within 63–81% SiO_2 range (Fig. 11). A characteristic feature of these tephras is that their glasses commonly form clusters or trends surrounded with large "halos" of scattered compositions (Fig. 11). In this study, we have tried to identify source volcanoes for distinct glass populations of the local tephras rather than for single shards.

The cindery tephras occur only in the lower part of the sections (Figs. 3 and 8). Glasses from these cinders ("local mafic glasses") fall mainly into the andesitic field with very few basaltic andesites (mostly tephra *PH7* and scattered shards at the bottom of K16-1 and KamPlen sections). Our reference compositions for mafic glasses include mostly Holocene tephras (Portnyagin et al., 2020), so we are not able to find exact matches for our late Pleistocene tephras in the proximal volcanic record. However, we identify four groups of mafic glasses, three of which resemble those from the Kliuchevskoi group volcanoes:

(1) *PH7* tephra from the Pakhcha valley is characterized by basaltic andesite, high-K, -Ti, and -P glass composition similar to that in the Holocene Tolbachik lava field cinders (Fig. 15A and B).
(2) Predominantly andesitic high-K, -Ti, and -P glasses are compositionally close to the Ushkovsky (Plosky) ones.
(3) Andesitic glasses with lower K and P contents fall into the Kliuchevskoi field.
(4) One more cluster of glasses with basaltic andesite to andesite high-K, -Ti, and –P compositions, which is most clearly defined by the SiO_2–P_2O_5 bi-plot (Fig. 15B). The glasses do not have matches in our database and seem to extend the trend formed by the medium-K Tolbachik glasses.

Glasses of group (1) are the youngest and occur only in the Pakhcha area; glasses of group (3) are most common in the cindery package at the bottom of the Kliuchi and KamPlen sections and are scattered in the sediments at the bottom of Pakhcha key site K16-18. Glasses from groups (2) and (4) are the oldest, and occur either at the very bottom of the cindery package or between *Gor28* and *Geys30* marker tephras. In the Kitilgina area, we found only two highly crystallized mafic tephras (*BY7* and *BY12*) with no pockets of fresh glass.

Glasses with SiO_2>63% from mineral-rich tephras ("local silicic glasses") have scattered low-to high-K compositions, but mostly falling in the medium-K field (Figs. 11 and 16A). Comparison to our database predictably suggests that these glasses are compositionally similar to known glasses from closely positioned Shiveluch (Young Shiveluch and Baidarny) and Zarechny volcanoes (Figs. 1, 2A and 16). However, the compositions of reference glass from Baidarny and Zarechny overlap and do not permit unique identification of tephra from each of these sources in our sections. To discriminate these tephras, we examined their phenocryst assemblages, glass morphology, and crystallinity (Supplement 1; Fig. 10).

Local silicic tephras in the KamPlen section exhibit the following

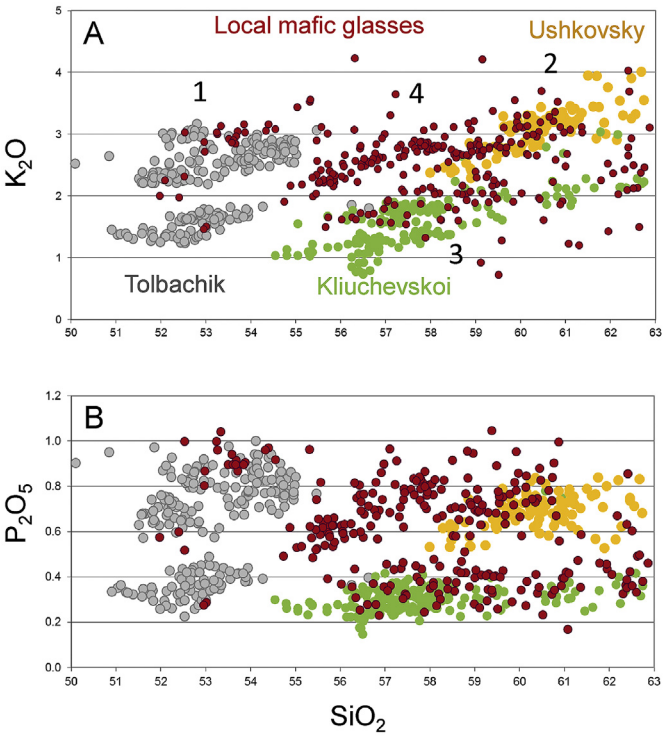

Fig. 15. Composition of mafic (SiO_2<63 wt%) glass from local mineral-rich tephras. Comparison of glasses from cindery mafic tephras from Kliuchi and Kozyrevsk study areas (red dots) with reference compositions for the Kliuchevskoi group volcanoes Tolbachik monogenetic lava field (gray), Ushkovsky (yellow) and Kliuchevskoi (green dots). The reference data is from TephraKam database (Portnyagin et al., 2020). 1–4 – four glass groups identified in the study area (see explanations in the text). Oxide concentrations are given in wt%. (For interpretation of the references to color in this figure legend, the reader is referred to the Web version of this article.)

mineral associations: (1) amphibole-plagioclase with rare pyroxenes (Pl > Amph ± Px), (2) two-pyroxene-plagioclase with rare olivine (Pl > Cpx + Opx ± Ol), and (3) two-pyroxene-amphibole with rare olivine and plagioclase (Amph > Cpx + Opx ± Ol > Pl) (Supplement 1).

(1) The presence of the first mineral association (Pl > Amph ± Px) and highly vesicular pumice shards (Fig. 10F) permits the confident identification of Young Shiveluch-type tephras (Figs. 3, 4 and 8). These characteristics are typical both for its Holocene (Ponomareva et al., 2015) and late Pleistocene activity (Gorbach et al., 2013).
(2) Pl > Cpx + Opx ± Ol association lacking amphibole is typical for the basaltic andesites of the Baidarny Spur and permits the identification of related tephras (Volynets et al., 1999; Gorbach et al., 2013).
(3) Tephras with high predominance of dark minerals (amphibole and pyroxenes) over plagioclase (Amph > Cpx + Opx ± Ol > Pl) are petrographically close to andesites of Zarechny volcano (Volynets et al., 1999b; Gorbach et al., 2018). In some very fine ash samples such as *KamPlen12* and *KamPlen14* (Fig. 3), plagioclase dominates over the dark minerals. However, the presence of amphibole allows us to distinguish these tephras from the Baidarny ones, and the large proportion of pyroxenes from the Shiveluch ones. In addition, a specific feature of Zarechny tephras is the presence of crystallized lithics petrographically identical to lavas of this volcano.

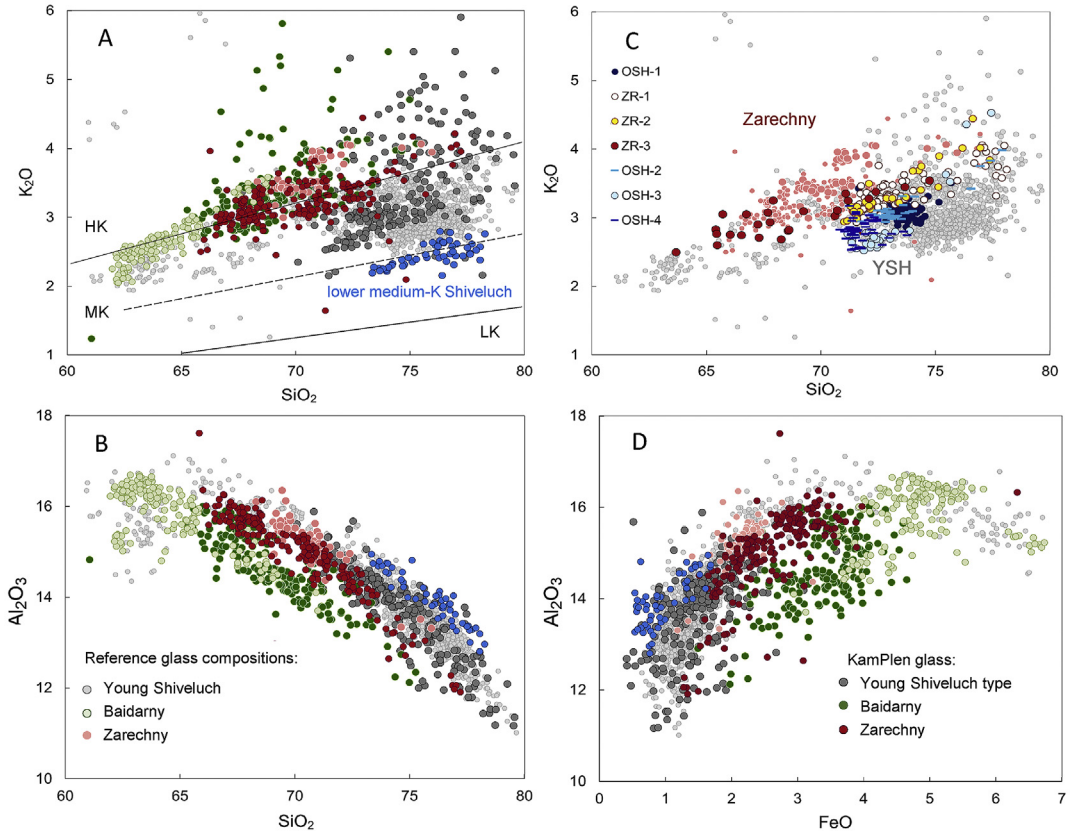

Fig. 16. Composition of silicic (SiO_2>65 wt%) glass from local mineral-rich tephras (**A, B, and D**) and composition of the marker tephras from the Shiveluch and Zarechny volcanoes (**C**). Comparison of silicic KamPlen glasses with reference compositions for local volcanoes Shiveluch (Young Shiveluch and Baidarny) and Zarechny. The reference data is from TephraKam database (Portnyagin et al., 2020). The tephra from study area are assigned to Young Shiveluch, Baidarny or Zarechny according to their mineral phenocryst assemblage (see explanations in the text). Oxide concentrations are given in wt%.

Discrimination of the Young Shiveluch-type, Baidarny, and Zarechny tephras based on their mineral assemblage permitted us to identify some distinctive features of their glass chemistry. Baidarny glasses have distinctively low Al_2O_3 at given SiO_2 or FeO (Fig. 16B and C). Zarechny and Young Shiveluch-type glasses partly overlap on all diagrams, but many presumably Zarechny glasses have lower SiO_2 and higher FeO in comparison with Shivelich glasses from the KamPlen section.

An interesting group of biotite-bearing Shiveluch tephras occurs only within the glacial package (Fig. 3 and Supplement 2, Fig. S7). Their glasses are lower in K_2O, TiO_2, and Cl, and higher in CaO and Al_2O_3 than those from typical Young Shiveluch tephra (Fig. 16). However, they match proximal intra-glacial pumices (Portnyagin et al., 2020), as well as distal tephras found east of the volcano directly below post-LGM fluvial deposits (Ponomareva et al., 2017). As such tephras do not occur in a well-resolved KamPlen or any other section southwest of the volcano, they cannot be precisely dated at this time. Absence of such tephras in the sections southwest of the volcano may be explained by dominantly eastern tephra dispersal at this time, as was, for example, the case of the YSH early Holocene tephras, which spread mostly to the east (Ponomareva et al., 2015).

Four Shiveluch (*OSH-1 – OSH-4*) and two or three Zarechny (*ZR-1 - ZR-3*) tephras were found in both Kliuchi and Kozyrevsk areas (Figs. 1, 3 and 86C). In Kitilgina, two compositionally identical Zarechny tephras occur in the upper part of the section (Fig. 3), and may represent either individual layers or a single layer duplicated due to redisposition. The wide dispersal of these tephras suggests that they can also be used as markers for Kliuchevskoi group and beyond (Table 2).

5. Discussion

5.1. Volcanological implications

Our tephra sequence combined from sixteen individual sections, linked through geochemically characterized marker layers, presents the first continuous pre-Holocene terrestrial record of explosive activity in Kamchatka spanning ~20 ka. Our sections capture tephras from all the Kamchatka volcanic zones (EVF, CKD, and SR), and even if they do not provide a complete tephra record for this time (as some of tephras might have been dispersed in other directions), they provide an important insight into the patterns of the late Pleistocene explosive activity in this region and tephrochronological framework for further studies.

5.1.1. Late Pleistocene record of large explosive eruptions in Kamchatka

Vitric tephras that occur both in Kliuchi-Kozyrevsk and Kitilgina areas – *EVF-1, EVF-2*, and *EVF-3*, and the marker triad composed of *Ber, Gor28*, and *Geys30* tephras (Table 2) – were likely produced by large eruptions. Indeed, the correlation of *Gor28* tephra to its proximal counterparts, Gorely caldera pumice, and to Ledovy Bluff in Chukotka (Fig. 1, inset), suggests its minimum volume estimate of ~40 km^3 (here and further on tephra volumes are based on single-isopach method by Legros, 2000), which corresponds to the eruption magnitude (M) ~6.5 (calculated according to Pyle et al., 1995). The other eruptions parental to vitric tephras yielded smaller

volumes of 7–20 km^3 although these estimates clearly may increase once their tephras are found farther afield. Our record shows that the large silicic explosive eruptions peaked starting from at least 30 ka to 25 ka (Fig. 8), however, as we do not have sediments older than ~30 ka, the start time of this eruptive peak remains unknown. Three large eruptions, which produced *Ber, Gor28*, and *Geys30* tephras occurred between 28.2 and 30 ka within a period of ~1.8 ka.

Our data show that the large late Pleistocene eruptions occurred nearly contemporaneously in the Eastern Volcanic Belt and Sredinny Range in Kamchatka. This is particularly well expressed by the triad of *Geis30*, *Gor28* and *Ber* tephras, which were erupted from VF, RA and SR, respectively. In comparison with the Holocene explosive activity including only one large eruption from SR volcanoes (Khangar eruption; Braitseva et al., 1997), late Pleistocene large eruptions from SR are more frequent (Table 2). These tephras were likely derived from the presently dormant volcanoes. This correlates with the overall waning volcanic activity in SR in the Holocene time (Ponomareva et al., 2007).

The tephra *BY10* has an exotic composition for Kamchatka (Figs. 14 and 15). Its distinctive features are low-K dacitic composition, low La/Y ~0.25, both typical for VF tephras, and relative enrichment in Nb (and Ta) so that the compositions have anomalously high Nb/Y ~0.15 and Nb/La ~0.6, which are significantly higher than typical values for the EVB magmas though all Pleistocene and Holocene (Fig. 14). Such high Nb/La are only known for SR magmas, which are however more enriched in all highly incompatible elements (i.e., LREE, Th, U, Ba, Rb). These geochemical features imply a relatively Nb–Ta undepleted magma source similar to primitive mantle (McDonough and Sun, 1995) and small contribution of high-Th/La and high-Th/Nb subducted sediments to the magma source (e.g. Plank, 2005; Duggen et al., 2007). Given the unusual composition, we have to assume that the *BY10* tephra comes either from previously unsampled Kamchatka volcano with atypical magma composition or from another arc, e.g. from the Western Aleutian Arc, where magmas originate at the conditions of highly oblique subduction and small sediment flux into the mantle wedge (e.g. Kelemen et al., 2003; Yogodzinski et al., 2015).

Our results provide another example of the earlier recognized clustering of the Kamchatka explosive eruptions during the Holocene time with a greater tendency to clustering for the largest events (Gusev et al., 2003), the pattern also seen in the Holocene global dataset (Gusev, 2008).

5.1.2. Late Pleistocene CKD volcanism

Tephra sequences in the northern part of our study area permit us to constrain the periods of explosive activity from Baidarny, Zarechny, Shiveluch and Bolshaya Udina volcanoes as well as activity of local mafic volcanoes (Figs. 1 and 2). In addition, they permit the dating of extensive megaplagiophyric basaltic trachyandesite lava flows outcropping along the Kamchatka River, which were produced from numerous monogenetic vents of the regional fissure zone superimposed on the Plosky volcanic massif (Supplement 4; Flerov et al., 2017). In Kliuchi sections, these lava flows are directly overlain by *Geys30* tephra so their age can be estimated at ~30 ka, which is close to an earlier estimate of 30–40 ka by Melekestsev et al. (1974) based on fresh topography of the lava surface and its relation with the LGM moraines. In the Pakhcha valley, lava flows of similar composition are overlain by both glacial tills or by lake deposits containing abundant glass shards from the marker tephra triad. In Pakhcha, the contact of tephra sequence and lava flows is not exposed, however, lava hummocks described in the Pakhcha riverbed (Kushev and Liverovsky, 1940) suggest the same young age of lava flows from the southern segment of the same fissure zone as in Kliuchi (Fig. 1).

Eruptions from Shiveluch volcano with tephra glasses compositionally similar to those from Young Shiveluch (presumably active from ~12.7 ka to present, Pevzner et al., 2013; Ponomareva et al., 2015) took place between ~27 and 17.5 ka (Fig. 8). This suggests that the Young Shiveluch-type melts were typical for Shiveluch in late Pleistocene as well, and thus what was thought to be the onset of Young Shiveluch activity was in fact a renewal of Shiveluch activity after a ~4.5 ka-long repose. The existence of a late Pleistocene eruptive vent now obscured by the younger deposits was suggested by Pevzner et al. (2018). The largest eruptions of the YSH-type tephras with volumes of ~0.3 km^3 took place at 18.6, 21.6, 26.2, and 26.3 ka (Fig. 8). Those were close to most of the Holocene YSH tephras in tephra volumes and dispersal distance suggesting a similar type of eruptive activity.

A specific low-K type of glasses from biotite-bearing Shiveluch tephras associated with its glacial deposits matches middle Pleistocene tephra WP11 (141–158 ka) found in the Bering Sea deposits (Derkachev et al., 2020), which suggests persistence of such melts in the Shiveluch history. Similar to our late Pleistocene tephra, the middle Pleistocene ash was also ejected during a cold marine isotope stage (MIS6) suggesting a possible link between this type of melts and glacial loading.

Late Pleistocene YSH-type of activity was succeeded by explosive activity from Baidarny vents, which persisted between ~17 and 11 ka and likely lasted intermittently into the Holocene (Ponomareva et al., 2015) or stopped at around 11.3 ka (Tolstykh et al., 2015). This age estimate is close to an earlier estimate of 16–11.3 ka (Pevzner et al., 2013). This is the only continuous episode of Baidarny activity since 30 ka BP, which might suggest this timing for its formation on the slope of Old Shiveluch volcano (Gorbach et al., 2013). Based on the dispersal of their tephras for $\leq$120 km (Figs. 3 and 8), Baidarny eruptions had moderate size with tephra volumes of <0.1 km^3.

The latest explosive activity from Zarechny volcano took place between 21.5 and 17 ka along with the YSH-type eruptions (Fig. 8) and was associated with Zarechny II volcano positioned in the collapse crater of the older Zarechny I edifice. Our age estimate significantly narrows an earlier suggested LGM age for Zarechny II activity (Volynets et al., 1999a). Most of Zarechny eruptions had moderate size with tephra volumes of <0.1 km^3. Only one or two Zarechny eruptions (*ZR-1* and *-2*) were larger and dispersed tephra to distances of ~190 km suggesting tephra volumes of ~0.2 km^3.

While Zarechny and YSH-type explosive activities are partly overlapping in time (between 21.5 and 17.5 ka), Baidarny activity succeeds both of them and is intercepted with only one distal *SVK-1* tephra from Sredinny Range (Fig. 8). Only four Shiveluch eruptions took place earlier than 25 ka BP, within the time interval dominated by silicic VF and SR tephras. This might suggest asynchronous activity from the CKD - and VF and SR volcanic zones.

All mafic tephras in the study area occur between 26 and 30 ka BP (Fig. 8). In Kliuchi and Kozyrevsk areas, they record the eruptions from at least four eruptive centers from local volcanoes (Fig. 15). The oldest cinders below *Gor28* likely record eruptions from the regional fissure zone superimposed on the Plosky volcanic massif and are probably related to the same eruptive episode as the lava flows in Kliuchi and Kozyrevsk areas (type 2 glass in Fig. 15A and B). Cindery package is composed mainly by Kliuchevskoi-type tephras (type 3); as Kliuchevskoi is believed to form in Holocene (Braitseva et al., 1995), this package suggests activity lasting for a few hundred years from an unknown volcano with similar glass compositions. In addition, glass types 1 and 4 likely record eruptions from Tolbachik eruptive centers.

BY13 tephra in Kitilgina area likely records a large eruption from Bolshaya Udina volcano at ~30 ka BP (Table 2; Fig. 8). This is the first age estimate for the activity of this volcano.

5.2. Paleogeographic implications

Global warming at the late Pleistocene and Holocene boundary caused dramatic and often rapid environmental changes. Abrupt climatic changes of this time are strongly pronounced in polar ice cores and marine sediments, but their effects in many terrestrial environments are still insufficiently understood due to scarcity of uninterrupted terrestrial records (e.g., Shakun and Carlson, 2010). For example, the extent and dynamics of the last glaciation in northeast Asia and the consequences of its decay for both land and adjacent waters are debatable (e.g., Gualtieri et al., 2000; Grosswald and Hughes, 2002; 2005; Brigham-Grette et al., 2003; Bigg et al., 2008). Northwest Pacific marine sediments around Kamchatka contain abundant ice-rafted debris (IRD) layers indicating large-scale glaciation (e.g., Bigg et al., 2008; Nürnberg et al., 2011; McCarron et al., 2020), as well as the evidence of repeated fresh water pulses, presumably associated with the Kamchatka glaciers decay (Gorbarenko et al., 2019). At the same time, terrestrial sediments that would provide a continuous and well-dated record of Pleistocene-Holocene environmental changes, are quite rare, which precludes the existence of a unified, consistent record of the dramatic environmental change during this time. Most existing studies of late Pleistocene glacial fluctuations in Kamchatka reconstruct two glacial stages (Braitseva et al., 1968; Melekestsev et al., 1974; Barr and Clark, 2012; Barr and Solomina, 2014) during the last 75 ka (Braitseva et al., 1995) or ~50 ka (Barr and Solomina, 2014). However, no robust age control for the terrestrial glacial deposits is available. Our study provides the first chronological control for glaciation-related deposits in the Central Kamchatka Depression (Figs. 1, 2 and 4).

5.2.1. Tephrochronological controls on glacial deposits

In our study area, we encountered two different groups of glacial deposits (Fig. 2B and C). The northern one is related to a large glacier originating from the Shiveluch collapse crater and extending for ~50 km down its southern slope across the modern Kamchatka River valley (Melekestsev et al., 1974, 1991b). Kliuchi area is located immediately southwest of its preserved moraine (Fig. 2B). Glaciofluvial deposits in Kliuchi contain exclusively andesitic material of Shiveluch affinity, reach thickness of >3 m and quickly pinch out westwards (Fig. 3 and Supplement 2, Fig. S7). The lowermost tephra layer on the top of these deposits is *SH#61a* (Ponomareva et al., 2015) with a KamPlen-modeled age of ~12 ka, which provides an upper limit for these deposits (Figs. 3 and 8). The lake deposits below the glaciofluvial package have been differentially eroded so the youngest of the preserved underlying tephras - *SVK-1* (~14.4 ka, Fig. 3) – might be somewhat older than the meltwater pulse.

The southern group of glacial deposits is exposed along the Pakhcha River and features two tills and two packages of glaciofluvial deposits (Figs. 2C, 4 and 6; Supplement 2, Figs S8 and S9; Kraevaya and Kuralenko, 1983). To date, this is the only place in Kamchatka where two late Pleistocene tills mapped by various researchers (e.g., Melekestsev et al., 1974; Barr and Clark, 2012; Barr and Solomina, 2014) are exposed in the same sections. M1 till is more massive and thicker, and extends farther than M2 (Kraevaya and Kuralenko, 1983). The youngest tephra underlying the younger M2 till is *OSH-1* dated at ~18.6 ka; this date provides a maximum estimate for the overlying M2 till. This means that the maximum advance of the younger Pakhcha glacier occurred somewhat later than the global LGM (24–18 ka BP; Mix et al., 2001).

The use of tephras overlying a glacial till in determining the age of glacial events might be problematic as their set may vary in different places due to various depositional conditions on the top of melting ice. However, we note that the oldest marker overlying the M1 till in section K16-2 (*OSH-3*, Fig. 4) also directly underlies glaciofluvial deposits in section K16-1 so this tephra might mark the waning of the M1 glacier at ~26.2 ka. Both M1 till and lacustrine deposits of the site K16-1 (where till is not present) overlie lava, however, their contact with lava is not exposed. Presence of the marker tephra triad glasses at the bottom of the lacustrine deposits suggests that the lava might be close in age to the Kliuchi one so the M1 till might be somewhat younger than 30 ka.

Clearly, our considerations are reconnaissance in character and the Pakhcha valley tills might reflect a local glacial story rather than a regional glaciation trend, however, our study provides the first ever attempt of the deciphering of late Pleistocene glacial history of the Kamchatka Peninsula with the help of tephrochronology.

Unlike the Pakhcha valley, the KamPlen site is located farther from glacier-filled paleovalleys (Fig. 2B). Changes in the KamPlen sedimentation rate might reflect changing climate/vegetation conditions in the basin rather than sediment input from an individual tributary. Sedimentation rate peaked at 24–21 ka and then at 19–17 ka (Fig. 8), probably reflecting increased erosion in cold times with reduced vegetation cover. Sharp increase of sedimentation rate at the bottom of the sequence is an artifact of modeling due to scarcity of model runs reaching bottom subsections (Bacon manual, Blaauw and Chrisen, http://www.chrono.qub.ac.uk/blaauw/manualBacon_2.3.pdf).

5.2.2. Was there a large MIS 2 paleolake in the Central Kamchatka Depression?

Previous studies described lacustrine deposits in different parts of the CKD. West of Kliuchi, such deposits were mentioned by Gushchenko (1965). In the Pakhcha valley, lacustrine deposits were described by Kraevaya (1977) and Kraevaya and Kuralenko (1983), who provided details of their structure, grain size, and mineral composition. A large massive of lacustrine deposits in the central part of CKD was described by Kushev and Liverovsky (1940) and Kuprina (1970). The latter study provides detailed description of the deposits as well as their grain size, mineral composition, and diatom assemblages. However, all these deposits have never been properly dated or correlated among the sites, which hampered the understanding of the extension of the lake basin.

Our longest tephra records in the Kliuchi, Pakhcha, and Kitilgina areas date back to 27–30 ka BP and are tightly linked by tephra markers (Fig. 8). In all these key sections - as well as in many shorter ones in our study - tephra-bearing deposits are mostly lacustrine in origin (Supplement 2, Figs. S2-S5). In this paper, we present only selected sites where most of the tephras have been analyzed, however, there are far more similar outcrops, which gave us an idea of continuity of the lacustrine deposits. For example, tephra sequences quite similar to that described in Kitilgina are (site 937) are exposed north of this site, along the Kitilgina River valley; sequences similar to KamPlen are exposed in other outcrops in the Kliuchi area; and the Pakhcha valley provides almost continuous outcrops of lacustrine and glacial deposits (Kraeveya and Kuralenko, 1983). This suggests that almost for 20 kyrs during MIS 2 most of the CKD functioned as a large lacustrine basin. The top of the highest lake deposits measured in our study has an elevation of ~150 m (Supplement 1). A 150 m isoline (Fig. 1) shows the minimum extent of the lake system. As there are no significant topographic barriers within the bounds of the reconstructed lake basin (Fig. 1), we suggest that, at least during some periods of the MIS 2, the CKD hosted a large, more or less continuous lake surface. Based on mapped configuration of Stage I glaciers (Fig. 2A), we suggest that an ice-dam is the most likely explanation for the paleolake formation. These MIS 2 ice bodies gained ground between 50 and 30 ka BP (Barr and Solomina, 2014) and extended around the Kliuchevskoi group and further north during this time

(Melekestsev et al., 1974, Fig. 2A).

The existence of a large glacial lake in the CKD is not surprising, as the depression is flanked on all sides by mountain ranges and has a quasi-closed nature. This is supported by the documentation of a large lake body within the CKD during the Middle Pleistocene (Braitseva et al., 1968, 2005). What is somewhat surprising is the apparent longevity of the MIS 2 glacial lake system (~20 ka), given that glacier-fed lakes tend to be short-lived (Ashley, 2002) and the host basin is volcanically and tectonically dynamic. This longevity might be explained by a specific geomorphology of the CKD pointing to highly constrained basin margin (Fig. 1), which would not allow frequent lake discharge and thus an ephemeral lake status. While the detailed spatial patterns of the Late Glacial ice margin retreat has yet to be resolved, the age of our terminal lacustrine deposits suggests that the MIS 2 glacial lake system in the Central Kamchatka Depression has lingered well into the Late Glacial and drained after the deposition of the ~12 ka *SH#61a* tephra.

5.2.3. Did melting of the LGM ice trigger enhanced silicic volcanism in Kamchatka?

Many authors agree that island-arc volcanic activity and large silicic eruptions, in particular, tend to peak few thousands years after deglaciation (e.g., Huybers and Langmuir, 2009; Kutterolf et al., 2013, 2019; Watt et al., 2013; Rawson et al., 2016). At the same time, a lack of well-resolved post-glacial volcanic records from different arcs hampers constraining global patterns in volcanic response to deglaciation (Watt et al., 2013).

Our detailed MIS 2 tephra record for Kamchatka explicitly shows that large silicic explosive eruptions peaked starting from at least 30 ka to 25 ka while the post-LGM deglaciation might have triggered only moderate Zarechny and minor basaltic andesite Baidarny activity (Fig. 8). One of the major explosive centers, Shiveluch volcano was active from at least 26.5 ka through the entire studied period - and into the Holocene times - with the periods of waning activity or quiescence from ~26 to 21.5 ka and from ~17.5 to 12 ka.

No large silicic eruptions have been found in our records in post-LGM time until an earlier documented peak of explosive silicic activity that started at ~9 ka BP (calibrated from Braitseva et al., 1995). The only large explosive eruption, which is known for the Late Glacial-early Holocene time, is PL2 from Plosky volcano. This eruption occurred at ~10.2 ka BP and produced basaltic andesite-andesite cinders with andesite glasses (Ponomareva et al., 2013).

The spectacular cluster of large silicic eruptions at 30–25 ka includes those from both major Kamchatka volcanic zones, EVB and SR, originating from both the southern (*Gor28*), central (*Geys30)* and northern (*Ber*) parts of the Kamchatka arc. This cluster - as well as massive lava outpouring from the regional fissure zone and cindery eruptions from at least four centers - occurred soon after the suggested 50–31 ka glacial advance (Barr and Solomina, 2014). However, as our record starts only at ~30 ka BP we do not know the start time of this eruptive cluster and cannot firmly link it to deglaciation.

6. Conclusions

This study presents the first continuous late Pleistocene tephrochronological record from Kamchatka Peninsula (Russian Far East) and one of the longest and best dated terrestrial tephra records in the North Pacific. This tephrochronological framework extends the existing continuous Holocene record of Kamchatka eruptions for ~20 millennia through the Last Glacial Maximum and the Late Glacial and has the potential to considerably enhance the integration of terrestrial and marine paleoenvironmental archives across the North Pacific, Beringia and beyond. The key findings of our research are summarized as follows:

1) The LGM-Late Glacial tephra record from Kamchatka Peninsula contains over 70 ash layers classified into two main groups: (1) dominantly vitric distal ashes representing large explosive eruptions from all major volcanic zones in Kamchatka, and (2) crystal-rich tephras largely from local volcanoes in the CKD, from both Kliuchevskoi and Shiveluch volcanic groups.
2) The Late Pleistocene tephrochronological model presented here is based on eleven AMS radiocarbon age measurements and contains 25 major tephra markers with an enhanced potential for regional and hemispheric correlations.
3) The tephrochronological framework allows valuable insights into local glacial history in the Kliuchevskoi volcanic group since 30 ka BP suggesting two glacial advance phases, at ~30 ka BP and after ~18 ka BP.
4) The most important landscape feature of this period is a newly proposed large glacial lake system that occupied over 10,000 km^2 of lowland between the Eastern and Sredinny Ranges of Kamchatka and deposited thick tephra-bearing lacustrine deposits over a period of almost 20 millennia until its final drainage around 12 ka BP.
5) The high quality geochemical and tephrochronological data presented here provide direct evidence for a nuanced Late Pleistocene eruptive history in one of the most active regions of the Pacific Ring of Fire. These data suggest a phase of strong explosive volcanism that started prior to 30 ka and ended ~25 ka BP, and was followed by a relative eruptive quiescence from ~25 to 21.5 ka BP and a moderate recrudescence from ~17.5 to 12 ka BP. The largest ($M \geq 6.5$) eruption within the 30–12 ka interval is associated with the Gorely eruptive center.

Authors statement

Vera Ponomareva: wrote the manuscript, conducted field work, collected tephra and sediment samples, conducted EMP analysis. I. Florin Pendea: wrote the manuscript, conducted field work, collected tephra and sediment samples, prepared samples and provided funding for 14C analysis. Egor Zelenin: wrote the manuscript, performed age modelling, tephra volume calculations, preparation of the graphic. Maxim Portnyagin: wrote the manuscript, performed LA-ICP-MS analysis and maintained databases of major and trace element glass compositions. Natalia Gorbach: wrote the manuscript, conducted field work, collected tephra and sediment samples, conducted mineralogical analysis and interpreted glass chemistry for local tephras. Maria Pevzner: conducted field work, collected tephra and sediment samples. Anastasia Plechova: conducted field work, collected tephra and sediment samples, conducted EMP analysis. Alexander Derkachev: provided his data on the Ber tephra in the Bering Sea sediments. Alexey Rogozin: conducted field work, collected tephra and sediment samples. Dieter Garbe-Schönberg: managed the LA-ICP-MS analyses. All authors discussed the results and participated in preparation of the paper

Declaration of competing interest

The authors declare that they have no known competing financial interests or personal relationships that could have appeared to influence the work reported in this paper.

Acknowledgements

This research was supported by the Russian Science Foundation

grant #16-17-10035 to Vera Ponomareva. Field work in Kitilgina area and Maria Pevzner's work on the manuscript were supported by her Russian Foundation for Basic Research grants #17-05-00352 and #20-05-00085. *Gor28* tephra sample from Chukotka was taken by late A.N. Kotov and was kindly provided by A.V. Lozhkin. Samples from core ODP145-883D were kindly provided by Grant Bigg; other samples from marine cores were obtained thanks to the German Federal Ministry for Education and Research (BMBF) KALMAR project. We are grateful to Paula Reimer and the ^{14}CHRONO Center of the Queen's University Belfast for providing the ^{14}C date for the proximal Gorely pumice. We acknowledge GEOMAR (Kiel, Germany) funding for the electron microprobe analyses and the Lakehead University Environmental lab in Orillia (Canada) for the preparation of radiocarbon samples. We thank Mario Thöner and Ulrike Westernströer for their assistance with electron probe and LA-ICP-MS analyses. One of the VP visits to the GEOMAR and Kiel University labs was supported by the German Academic Exchange Service (DAAD). The authors thank Sofia Garipova for her help with graphic representation of maps. We are thankful to two anonymous reviewers who provided detailed comments on the manuscript allowing the authors to refine their results.

Appendix A. Supplementary data

Supplementary data to this article can be found online at https://doi.org/10.1016/j.quascirev.2021.106838.

References

Albert, P.G., Smith, V.C., Suzuki, T., McLean, D., Tomlinson, E.L., Miyabuchi, Y., Kitaba, I., Mark, D.F., Moriwaki, H., Members, S.P., Nakagawa, T., 2019. Geochemical characterisation of the Late Quaternary widespread Japanese tephrostratigraphic markers and correlations to the Lake Suigetsu sedimentary archive (SG06 core). Quat. Geochronol. 52, 103–131.

Ashley, G.M., 2002. Glaciolacustrine environments. Modern and Past Glacial Environments. Butterworth-Heinemann, pp. 335–359.

Barr, I.D., Clark, C.D., 2012. Late Quaternary glaciations in Far NE Russia; combining moraines, topography and chronology to assess regional and global glaciation synchrony. Quat. Sci. Rev. 53, 72–87.

Barr, I.D., Solomina, O., 2014. Pleistocene and holocene glacier fluctuations upon the Kamchatka peninsula. Global Planet. Change 113, 110–120. https://doi.org/10.1016/j.gloplacha.2013.08.005.

Bazanova, L.I., Braitseva, O.A., Dirksen, O.V., Sulerzhitsky, L.D., Danhara, T., 2005. Ashfalls from the largest Holocene eruptions along the Ust'-Bol'sheretsk-Petropavlovsk-Kamchatsky traverse: sources, chronology, recurrence. Volcanol. Seism. 6, 30–46 (in Russian).

Bigg, G.R., Clark, C.D., Hughes, A.L.C., 2008. A last glacial ice sheet on the Pacific Russian coast and catastrophic change arising from coupled ice-volcanic interaction. Earth Planet Sci. Lett. 265, 559–570. https://doi.org/10.1016/j.epsl.2007.10.052.

Bindeman, I.N., Leonov, V.L., Izbekov, P.E., Ponomareva, V.V., Watts, K.E., Shipley, N.K., Perepelov, A.B., Bazanova, L.I., Jicha, B., Singer, B.S., Schmitt, A.K., Portnyagin, M.V., Chen, C.H., 2010. Large-volume silicic volcanism in Kamchatka: Ar-Ar and U-Pb ages, isotopic, and geochemical characteristics of major pre-Holocene caldera-forming eruptions. J. Volcanol. Geoth. Res. 189, 57–80. https://doi.org/10.1016/j.jvolgeores.2009.10.009.

Blaauw, M., Christen, J.A., 2011. Flexible paleoclimate age-depth models using an autoregressive gamma process. Bayesian Anal 6, 457–474. https://doi.org/10.1214/11-BA618.

Braitseva, O.A., Melekestsev, I.V., Evteeva, J.S., Lupikina, E.G., 1968. Stratigraphy of Quaternary Deposits and Glaciations of Kamchatka. Nauka, Moscow, p. 227 (in Russian).

Braitseva, O.A., Melekestsev, I.V., Ponomareva, V.V., Sulerzhitsky, L.D., 1995. Ages of calderas, large explosive craters and active volcanoes in the Kuril-Kamchatka region, Russia. Bull. Volcanol. 57, 383–402. https://doi.org/10.1007/BF00300984.

Braitseva, O.A., Ponomareva, V.V., Sulerzhitsky, L.D., Melekestsev, I.V., Bailey, J., 1997. Holocene key-marker tephra layers in Kamchatka, Russia. Quat. Res. 47, 125–139. https://doi.org/10.1006/qres.1996.1876.

Braitseva, O.A., Melekestsev, I.V., Sulerzhitsky, L.D., 2005. New data on the Pleistocene deposits age in the Central Kamchatka depression. Stratigr. Geol. Correl. 13, 99–107.

Brigham-Grette, J., Gualtieri, L.M., Glushkova, O.Y., Hamilton, T.D., Mostoller, D., Kotov, A., 2003. Chlorine-36 and 14C chronology support a limited last glacial maximum across central Chukotka, northeastern Siberia, and no Beringian ice sheet. Quat. Res. 59 (3), 386–398. https://doi.org/10.1016/S0033-5894(03)00058-9.

Bronk Ramsey, C., 2009. Bayesian analysis of radiocarbon dates. Radiocarbon 51, 337–360. https://doi.org/10.1017/s0033822200033865.

Bronk Ramsey, C., 2008. Deposition models for chronological records. Quat. Sci. Rev. 27, 42–60. https://doi.org/10.1016/j.quascirev.2007.01.019.

Bronk Ramsey, C., Lee, S., 2013. Recent and planned developments of the program OxCal. Radiocarbon 55, 720–730. https://doi.org/10.1017/S0033822200057878.

Churikova, T., Dorendorf, F., Wörner, G., 2001. Sources and fluids in the mantle wedge below Kamchatka, evidence from across-arc geochemical variation. J. Petrol. 42 (8), 1567–1593.

Cook, E., Portnyagin, M.V., Ponomareva, V.V., Bazanova, L.I., Svensson, A., Garbe-Schönberg, D., 2018. First identification of cryptotephra from the Kamchatka Peninsula in a Greenland ice core: implications of a widespread marker deposit that links Greenland to the Pacific northwest. Quat. Sci. Rev. 181, 200–206. https://doi.org/10.1016/j.quascirev.2017.11.036.

Davies, L.J., Jensen, B.J., Froese, D.G., Wallace, K.L., 2016. Late Pleistocene and Holocene tephrostratigraphy of interior Alaska and Yukon: key beds and chronologies over the past 30,000 years. Quat. Sci. Rev. 146, 28–53.

Derkachev, A.N., Nikolaeva, N.A., Gorbarenko, S.A., Portnyagin, M.V., Ponomareva, V.V., Nürnberg, D., Sakamoto, T., Iijima, K., Liu, Y., Shi, X., Lv, H., Wang, K., 2016. Tephra layers of in the quaternary deposits of the Sea of Okhotsk: distribution, composition, age and volcanic sources. Quat. Int. 425, 248–272. https://doi.org/10.1016/j.quaint.2016.07.004.

Derkachev, A.N., Gorbarenko, S.A., Ponomareva, V.V., Portnyagin, M.V., Malakhova, G.I., Liu, Y., 2020. Middle to late Pleistocene record of explosive volcanic eruptions in marine sediments offshore Kamchatka (Meiji Rise, NW Pacific). J. Quat. Sci. 35, 362–379. https://doi.org/10.1002/jqs.3175.

Dikov, N.N., 2003. Archaeological Sites of Kamchatka, Chukotka, and the Upper Kolyma. Shared Beringian Heritage Program, Anchorage, p. 394.

Duggen, S., Portnyagin, M., Baker, J., Ulfbeck, D., Hoernle, K., Garbe-Schönberg, D., Grassineau, N., 2007. Drastic shift in lava geochemistry in the volcanic-front to rear-arc region of the Southern Kamchatkan subduction zone: evidence for the transition from slab surface dehydration to sediment melting. Geochem. Cosmochim. Acta 71, 452–480.

Dullo, W.-C., Baranov, B., van den Bogaard, C., 2009. FS Sonne Fahrtbericht/Cruise Report SO201-2 KALMAR: Kurile-Kamchatka and ALeutian MARginal Sea-Island Arc Systems: Geodynamic and Climate Interaction in Space and Time. Busan/Korea-Tomakomai/Japan, 30.08.-08.10. 2009.

Flerov, G.B., Churikova, T., Anan'ev, V.V., 2017. The Ploskie sopki volcanic massif: geology, petrochemistry, mineralogy, and petrogenesis (Klyuchevskoi volcanic cluster, Kamchatka). J. Volcanol. Seismol. 11, 266–284. https://doi.org/10.1134/S0742046317040030.

Fontijn, K., Rawson, H., Van Daele, M., Moernaut, J., Abarzúa, A.M., Heirman, K., Bertrand, S., Pyle, D.M., Mather, T.A., De Batist, M., Naranjo, J.A., 2016. Synchronisation of sedimentary records using tephra: a postglacial tephrochronological model for the Chilean Lake District. Quat. Sci. Rev. 137, 234–254.

Goebel, T., Slobodin, S.B., Waters, M.R., 2010. New dates from Ushki-1, Kamchatka, confirm 13,000calBP age for earliest Paleolithic occupation. J. Archaeol. Sci. 37, 2640–2649. https://doi.org/10.1016/j.jas.2010.05.024.

Goebel, T., Waters, M.R., Dikova, M., 2003. The archaeology of Ushki lake, Kamchatka, and the Pleistocene peopling of the americas. Science 84 301, 501–505. https://doi.org/10.1126/science.1086555.

Gorbach, N., Portnyagin, M.V., Tembrel, I., 2013. Volcanic structure and composition of Old Shiveluch volcano, Kamchatka. J. Volcanol. Geoth. Res. 263, 193–208. https://doi.org/10.1016/j.jvolgeores.2012.12.012.

Gorbach, N., Ponomareva, V.V., Pendea, I.F., Portnyagin, M.V., 2018. Small but important: new data about activity and composition of Zarechny volcano (Central Kamchatka Depression). In: 10th Biennual Workshop on Japan-Kamchatka-Alaska Subduction Processes (JKASP-2018). Petropavlovsk-Kamchatsky, Russia, pp. 83–85. http://www.kscnet.ru/ivs/conferences/jkasp2018/pdf/GorbachNV_66-36.pdf.

Gorbarenko, S.A., Shi, X., Zou, J., Velivetskaya, T., Artemova, A., Liu, Y., Yanchenko, E., Vasilenko, Y., 2019. Evidence of meltwater pulses into the north pacific over the last 20 ka due to the decay of Kamchatka glaciers and cordilleran ice sheet. Global Planet. Change 172, 33–44. https://doi.org/10.1016/j.gloplacha.2018.09.014.

Gorbatov, A., Kostoglodov, V., Suárez, G., Gordeev, E.I., 1997. Seismicity and structure of the Kamchatka subduction zone. J. Geophys. Res. Solid Earth 102, 17883–17898. https://doi.org/10.1029/96jb03491.

Grosswald, M.G., Hughes, T.J., 2002. The Russian component of an arctic ice sheet during the last glacial maximum. Quat. Sci. Rev. 21, 121–146. https://doi.org/10.1016/S0277-3791(01)00078-6.

Grosswald, M.G., Hughes, T.J., 2005. "Back-arc" marine ice sheet in the Sea of Okhotsk. Russ. J. Earth Sci. 7 https://doi.org/10.2205/2005ES000180.

Gualtieri, L., Glushkova, O., Brigham-Grette, J., 2000. Evidence for restricted ice extent during the last glacial maximum in the Koryak Mountains of Chukotka, far Eatern Russia. Bull. Geol. Soc. Am. 112, 1106–1118. https://doi.org/10.1130/0016-7606(2000)112<1106:EFRIED>2.0.CO;2.

Gusev, A.A., Ponomareva, V.V., Braitseva, O.A., Melekestsev, I.V., Sulerzhitsky, L.D., 2003. Great explosive eruptions on Kamchatka during the last 10,000 years: self-similar irregularity of the output of volcanic products. J. Geophys. Res. Solid Earth 108/B2, 2126. https://doi.org/10.1029/2001JB000312.

Gusev, A.A., 2008. Temporal structure of the global sequence of volcanic eruptions: order clustering and intermittent discharge rate. Phys. Earth Planet. In. 166, 203–218. https://doi.org/10.1016/j.pepi.2008.01.004.
Gushchenko, I.I., 1965. Ashes from North Kamchatka and Conditions of Their Formation. Nauka, Moscow, p. 143 (in Russian).
Huybers, P., Langmuir, C., 2009. Feedback between deglaciation, volcanism, and atmospheric CO_2. Earth Planet Sci. Lett. 286, 479–491. https://doi.org/10.1016/j.epsl.2009.07.014.
Kelemen, P.B., Yogodzinski, G.M., Scholl, D.W., 2003. Along-Strike Variations in the Aleutian Island Arc: Genesis of High Mg# Andesite and Implications for Continental Crust, inside the Subduction Factory. American Geophysical Union, pp. 223–276.
Kirianov, V.Yu, 1981. About the possibility of correlation of ash horizons in the Pleistocene deposits of the Central Kamchatka Depression. Volcanol. Seismol. 6, 30–38 (in Russian).
Kotov, A.N., Lozhkin, A.V., Ryabchun, V.K., 1989. Permafrost-facial conditions of the upper Pleistocene deposit creation of the main river valley (Chukotka). In: Ivanov, V.F., Palymsky, B.F. (Eds.), Forming of Relief, Correlated Deposit and Gravels of the Northern-East of USSR. SVKNII DVO AS USSR, Magadan, pp. 117–131 (in Russian).
Kraevaya, T.S., 1977. Genetic Types of Coarse-Clastic Deposits at Stratovolcanoes. Nedra, Moscow, p. 126 (in Russian).
Kraevaya, T.S., Kuralenko, N.P., 1983. Upper Pleistocene glacial deposits at foothills of active volcanoes of Kamchatka. Volcanol. Seismol. 25–35 (in Russian).
Kuprina, N., 1970. Stratigraphy and History of Pleistocene Sedimentation in Central Kamchatka. Nauka, Moscow, p. 150 (in Russian).
Kushev, S.L., Liverovsky, Y.A., 1940. Geomorphological Sketch of the Central Kamchatka Depression. AN USSR, Moscow, p. 85 (in Russian).
Kutterolf, S., Jegen, M., Mitrovica, J.X., Kwasnitschka, T., Freundt, A., Huybers, P.J., 2013. A detection of Milankovitch frequencies in global volcanic activity. Geology 41 (2), 227–230. https://doi.org/10.1130/G33419.1.
Kutterolf, S., Schindlbeck, J.C., Jegen, M., Freundt, A., Straub, S.M., 2019. Milankovitch frequencies in tephra records at volcanic arcs: the relation of kyr-scale cyclic variations in volcanism to global climate changes. Quat. Sci. Rev. 204, 1–16. https://doi.org/10.1016/j.quascirev.2018.11.004.
Kyle, P.R., Ponomareva, V.V., Rourke Schluep, R., 2011. Geochemical characterization of marker tephra layers from major Holocene eruptions, Kamchatka Peninsula, Russia. Int. Geol. Rev. 53, 1059–1097. https://doi.org/10.1080/00206810903442162.
Legros, F., 2000. Minimum volume of a tephra fallout deposit estimated from a single isopach. J. Volcanol. Geoth. Res. 96, 25–32. https://doi.org/10.1016/S0377-0273(99)00135-3.
Le Maitre, R.W., Streckeisen, A., Zanetti, B., Le Bas, M.J., Bonin, B., Bateman, P., Bellieni, G., Dudek, A., Efremova, S., Keller, J., Lameyre, J., Sabine, P.A., Schmid, R., Soerensen, H., Wooley, A.R. (Eds.), 2002. Igneous Rocks. A Classification and Glossary of Terms. Cambridge University Press.
Mackay, H., Hughes, P.D.M., Jensen, B.J.L., Langdon, P.G., Pyne-O'Donnell, S.D.F., Plunkett, G., Froese, D.G., Coulter, S., Gardner, J.E., 2016. A mid to late Holocene cryptotephra framework from eastern North America. Quat. Sci. Rev. 132, 101–113. https://doi.org/10.1016/j.quascirev.2015.11.011.
McCarron, A.P., Bigg, G.R., Brooks, H., Leng, M.J., Marshall, J.D., Ponomareva, V.V., Portnyagin, M.V., Reimer, P.J., Rogerson, M., 2020. Northwest Pacific ice-rafted debris at 38°N reveals episodic ice-sheet change in late Quaternary Northeast Siberia. Earth Planet. Sci. Lett. In revision.
McDonough, W.F., Sun, S.-S., 1995. The composition of the Earth. Chem. Geol. 120, 223–253.
Melekestsev, I.V., 1974. Major stages of the formation of modern relief of the Kurile-Kamchatka region. In: Luchitsky, I.V. (Ed.), Kamchatka, Kurile and Commander Islands. Nauka, Moscow, pp. 337–344 (in Russian).
Melekestsev, I.V., Braitseva, O.A., Erlich, E.N., Kozhemyaka, N.N., 1974. Volcanic mountains and plains. In: Luchitsky, I.V. (Ed.), Kamchatka, Kurile and Commander Islands. Nauka, Moscow, pp. 162–234 (in Russian).
Melekestsev, I.V., Glushkova, O.Y., Kirianov, V.Y., Lozhkin, A.V., Sulerzhitsky, L.D., 1991a. Age and origin of Magadan ashes. Proc. USSR Acad. Sci. 317, 1188–1192 (in Russian).
Melekestsev, I.V., Volynets, O.N., Ermakov, V.A., Kirsanova, T.P., Masurenkov, Y.P., 1991b. Shiveluch volcano. In: Fedotov, S.A., Masurenkov, Yu P. (Eds.), Active Volcanoes of Kamchatka. Nauka, Moscow, pp. 84–103 (in Russian, summary in English).
Melekestsev, I.V., Litasova, S.N., Sulerzhitsky, L.D., 1992. On the age and scale of the directed-blast catastrophic eruption of the Avachinsky volcano (Kamchatka) in the Late Pleistocene. Volcanol. Seismol. 13 (2), 135–146.
Mix, A.C., Bard, E., Schneider, R., 2001. Environmental processes of the ice age: land, oceans, glaciers (EPILOG). Quat. Sci. Rev. 20 (4), 627–657. https://doi.org/10.1016/S0277-3791(00)00145-1.
Nürnberg, D., Dethleff, D., Tiedemann, R., Kaiser, A., Gorbarenko, S.A., 2011. Okhotsk Sea ice coverage and Kamchatka glaciation over the last 350ka - evidence from ice-rafted debris and planktonic α18O. Palaeogeogr. Palaeoclimatol. Palaeoecol. 310, 191–205. https://doi.org/10.1016/j.palaeo.2011.07.011.
Ogorodov, N.V., Kozhemyaka, N.N., Vazheevskaya, A.A., Ogorodova, A.S., 1972. Volcanoes and Quaternary Volcanism of the Sredinny Ridge of Kamchatka. Nauka, Moscow, p. 191 (in Russian).
Pevzner, M.M., Ponomareva, V.V., Sulerzhitsky, L.D., 2006. Holocene soil-pyroclastic cover of the Central Kamchatka Depression: age, structure, sedimentation patterns. Volcanol. Seismol. 1, 24–38 (in Russian).
Pevzner, M.M., 2015. Holocene Volcanism of Srediiny Range of Kamchatka. GEOS, Moscow, p. 252 (in Russian).
Pevzner, M.M., Babanskii, A.D., Tolstykh, M.L., Kononkova, N.N., 2013. Reconstruction of the magmatic system in the Shiveluch volcanic massif as a result of large-scale collapses of its edifice in the late Pleistocene-early Holocene. In: Doklady Earth Sciences, pp. 35–37. https://doi.org/10.1134/S1028334X1210011X.
Pevzner, M.M., Tolstykh, M.L., Babansky, A.D., 2018. The Shiveluch Volcanic Massif, Kamchatka: stages in the evolution of a magmatic system: results of geochronological and thermobarogeochemical Studies. J. Volcanol. Seismol. 12 (4), 242–251.
Pinegina, T.K., Bazanova, L.I., Zelenin, E.A., Bourgeois, J., Kozhurin, A.I., Medvedev, I.P., Vydrin, D.S., 2018. Holocene tsunamis in avachinsky bay, Kamchatka, Russia. Pure Appl. Geophys. 175 (4), 1485–1506.
Pinegina, T.K., Bourgeois, J., Bazanova, L.I., Zelenin, E.A., Krasheninnikov, S.P., Portnyagin, M.V., 2020. Coseismic coastal subsidence associated with unusually wide rupture of prehistoric earthquakes on the Kamchatka subduction zone: a record in buried erosional scarps and tsunami deposits. Quat. Sci. Rev. 233, 106171.
Plank, T., 2005. Constraints from thorium/lanthanum on sediment recycling at subduction zones and the evolution of the continents. J. Petrol. 46, 921–944.
Ponomareva, V.V., Kyle, P.R., Melekestsev, I.V., Rinkleff, P.G., Dirksen, O.V., Sulerzhitsky, L.D., Zaretskaia, N.E., Rourke, R., 2004. The 7600 (14C) year BP Kurile Lake caldera-forming eruption, Kamchatka, Russia: stratigraphy and field relationships. J. Volcanol. Geoth. Res. 136, 199–222. https://doi.org/10.1016/j.jvolgeores.2004.05.013.
Ponomareva, V.V., Churikova, T.G., Melekestsev, I.V., Braitseva, O.A., Pevzner, M.M., Sulerzhitsky, L.D., 2007. Late pleistocene-holocene volcanism on the Kamchatka peninsula, northwest pacific region. In: Eichelberger, J., Gordeev, E., Kasahara, M., Izbekov, P., Lees, J. (Eds.), Volcanism and Subduction: the Kamchatka Region, vol. 172. American Geophysical Union Geophysical Monograph Series, pp. 165–198.
Ponomareva, V.V., Portnyagin, M.V., Derkachev, A.N., Juschus, O., Garbe-Schönberg, D., Nürnberg, D., 2013a. Identification of a widespread Kamchatkan tephra: a middle Pleistocene tie-point between Arctic and Pacific paleoclimatic records. Geophys. Res. Lett. 40, 3538–3543. https://doi.org/10.1002/grl.50645.
Ponomareva, V.V., Portnyagin, M.V., Derkachev, A.N., Pendea, I.F., Bourgeois, J., Reimer, P.J., Garbe-Schönberg, D., Krasheninnikov, S., Nürnberg, D., 2013b. Early Holocene M~6 explosive eruption from Plosky volcanic massif (Kamchatka) and its tephra as a link between terrestrial and marine paleoenvironmental records. Int. J. Earth Sci. 102/6, 1673–1699. https://doi.org/10.1007/s00531-013-0898-0.
Ponomareva, V.V., Portnyagin, M.V., Pevzner, M.M., Blaauw, M., Kyle, P.R., Derkachev, A.N., 2015. Tephra from andesitic Shiveluch volcano, Kamchatka, NW Pacific: chronology of explosive eruptions and geochemical fingerprinting of volcanic glass. Int. J. Earth Sci. 104, 1459–1482. https://doi.org/10.1007/s00531-015-1156-4.
Ponomareva, V.V., Portnyagin, M.V., Pendea, I.F., Zelenin, E.A., Bourgeois, J., Pinegina, T.K., Kozhurin, A.I., 2017. A full holocene tephrochronology for the kamchatsky peninsula region: applications from Kamchatka to north America. Quat. Sci. Rev. 168, 101–122. https://doi.org/10.1016/j.quascirev.2017.04.031.
Portnyagin, M.V., Ponomareva, V.V., Zelenin, E.A., Bazanova, L.I., Pevzner, M.M., Plechova, A.A., Rogozin, A.N., Garbe-Schönberg, Di, 2020. TephraKam: geochemical database of glass compositions in tephra and welded tuffs from the Kamchatka volcanic arc (northwestern Pacific). Earth Syst. Sci. Data 12, 469–486. https://doi.org/10.5194/essd-12-469-2020.
Pyle, D.M., 1995. Assessment of the minimum volume of tephra fall deposits. J. Volcanol. Geoth. Res. 69, 379–382. https://doi.org/10.1016/0377-0273(95)00038-0.
Reimer, P.J., Bard, E., Bayliss, A., Beck, J.W., Blackwell, P.G., Bronk Ramsey, C., Buck, C.E., Cheng, H., Edwards, R.L., Friedrich, M., Grootes, P.M., Guilderson, T.P., Haflidason, H., Hajdas, I., Hatté, C., Heaton, T.J., Hoffmann, D.L., Hogg, A.G., Hughen, K.A., Kaiser, K.F., Kromer, B., Manning, S.W., Niu, M., Reimer, R.W., Richards, D.A., Scott, E.M., Southon, J.R., Staff, R.A., Turney, C.S.M., van der Plicht, J., 2013. IntCal13 and Marine13 radiocarbon age calibration curves 0–50,000 Years cal BP. Radiocarbon 55, 1869–1887. https://doi.org/10.2458/azu_js_rc.55.16947.
Riethdorf, J.R., Nürnberg, D., Max, L., Tiedemann, R., Gorbarenko, S.A., Malakhov, M.I., 2013. Millennial-scale variability of marine productivity and terrigenous matter supply in the western Bering Sea over the past 180 kyr. Clim. Past 9 (3), 1345–1373.
Selyangin, O.B., Ponomareva, V.V., 1999. Gorelovsky volcanic center, South Kamchatka: structure and evolution. Volcanol. Seismol. 21, 163–194.
Shakun, J.D., Carlson, A.E., 2010. A global perspective on Last Glacial Maximum to Holocene climate change. Quat. Sci. Rev. 29, 1801–1816. https://doi.org/10.1016/j.quascirev.2010.03.016.
Solomina, O., Wiles, G., Shiraiwa, T., D'Arrigo, R., 2007. Multiproxy records of climate variability for Kamchatka for the past 400 years. Clim. Past 3, 119–128. https://doi.org/10.5194/cp-3-119-2007.
Tolstykh, M.L., Pevzner, M.M., Naumov, V.B., Babanskii, A.D., Kononkova, N.N., 2015. Types of parental melts of pyroclastic rocks of various structural–age complexes of the Shiveluch volcanic massif, Kamchatka: evidence from inclusions in minerals. Petrology 23, 480–517. https://doi.org/10.1134/S0869591115040050.
van der Bilt, W.G.M., Lane, C.S., Bakke, J., 2017. Ultra-distal Kamchatkan ash on Arctic Svalbard: towards hemispheric cryptotephra correlation. Quat. Sci. Rev. 164, 230–235. https://doi.org/10.1016/j.quascirev.2017.04.007.

Volynets, O.N., 1994. Geochemical types, petrology, and genesis of late cenozoic volcanic rocks from the Kurile-Kamchatka Island-arc system. Int. Geol. Rev. 36, 373–405. https://doi.org/10.1080/00206819409465467.

Volynets, O.N., Ponomareva, V.V., Babansky, A.D., 1997. Magnesian basalts of Shiveluch andesite volcano, Kamchatka. Petrology 5 (2), 183–196.

Volynets, O.N., Melekestsev, I.V., Ponomareva, V.V., Yogodzinski, G.M., 1999a. Kharchinsky and Zarechnyi volcanoes - unique centers of late Pleistocene magnesian basalts in Kamchatka: structural setting, morphology, geologic structure and age. Volcanol. Seismol. 20, 383–399.

Volynets, O.N., Melekestsev, I.V., Ponomareva, V.V., Yogodzinski, J.M., 1999b. Kharchinskii and Zarechnyi volcanoes, unique centers of Late Pleistocene magnesian basalts in Kamchatka: composition of erupted rocks. Volcanol. Seismol. 21, 45–66.

Watt, S.F.L., Pyle, D.M., Mather, T.A., 2013. The volcanic response to deglaciation: evidence from glaciated arcs and a reassessment of global eruption records. Earth Sci. Rev. 122, 77–102. https://doi.org/10.1016/j.earscirev.2013.03.007.

Yogodzinski, G.M., Brown, S.T., Kelemen, P.B., Vervoort, J.D., Portnyagin, M., Sims, K.W.W., Hoernle, K., Jicha, B.R., Werner, R., 2015. The role of subducted basalt in the source of island arc magmas: evidence from seafloor lavas of the western aleutians. J. Petrol. 56, 441–492.

Zelenin, E.A., Kozhurin, A.I., Ponomareva, V.V., Portnyagin, M.V., 2020. Tephrochronological dating of paleoearthquakes in active volcanic arcs: a case of the Eastern Volcanic Front on the Kamchatka Peninsula (northwest Pacific). J. Quat. Sci. 35, 349–361. https://doi.org/10.1002/jqs.3145.